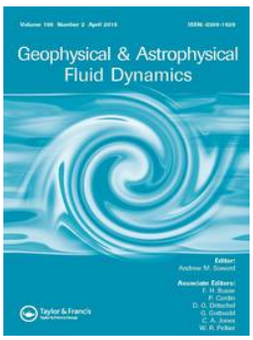

Geophysical & Astrophysical Fluid Dynamics

ISSN: 0309-1929 (Print) 1029-0419 (Online) Journal homepage: http://www.tandfonline.com/loi/ggaf20

On the combined effect of atmospheric stratification and non-uniform magnetic field on magneto-sonic-gravity waves

L. M. B. C. Campos & A. C. Marta

To cite this article: L. M. B. C. Campos & A. C. Marta (2015) On the combined effect of atmospheric stratification and non-uniform magnetic field on magneto-sonic-gravity waves, Geophysical & Astrophysical Fluid Dynamics, 109:2, 168-198, DOI: 10.1080/03091929.2015.1032959

To link to this article: http://dx.doi.org/10.1080/03091929.2015.1032959

Geophysical and Astrophysical Fluid Dynamics, 2015
Vol. 109, No. 2, 168–198, http://dx.doi.org/10.1080/03091929.2015.1032959

Taylor & Francis
Taylor & Francis Group

On the combined effect of atmospheric stratification and non-uniform magnetic field on magneto-sonic-gravity waves

L. M. B. C. CAMPOS and A. C. MARTA*

CCTAE, IDMEC, Instituto Superior Técnico, Universidade de Lisboa, 1049-001 Lisboa, Portugal

(*Received 19 June 2014; in final form 10 March 2015*)

The linear magneto-acoustic-gravity (MAG) wave equation is considered for a non-isothermal atmosphere under a non-uniform external magnetic field. The starting point is a magnetohydrostatic equilibrium with an arbitrary profiles of temperature and horizontal magnetic field as a function of altitude; this specifies the profiles of gas pressure, mass density and sound and Alfvén speeds. The wave equation is solved exactly in the case of an isothermal atmosphere with horizontal magnetic field decaying exponentially with altitude on twice the scale height. The solution for the vertical velocity perturbation is represented by confluent hypergeometric functions specifying the effect of the magnetic field in modifying the amplitude and phase of acoustic-gravity waves. It is shown that (i) in the physical conditions corresponding to the solar corona, the decrease in Alfvén speed with height leads to a decreasing spacing of nodes; this agrees with observations of ratios of periods p_2/p_1 less than two in solar arches or loops; also (ii) the dissipation of these magnetosonic-gravity modes in the solar transition region is sufficient to heat the corona by compensating for energy losses in solar radiation. (i) and (ii) are set in the context of a tentative global picture of the possible role of MAG waves in establishing the mass and energy balances in the solar atmosphere.

Keywords: Magnetohydrodynamics; Waves; Sun; Stellar atmospheres

1. Introduction

The original suggestion that the dissipation of acoustic (Biermann 1948, Schwarzschild 1948) or hydromagnetic (Alfvén 1947, Alfvén 1950) waves could heat the solar atmosphere started a large body of research of magneto-atmospheric waves (see reviews by Thomas 1983, Campos 1987, Roberts 2000) related to ground-based and satellite observations (e.g. Banerjee *et al.* 2007, Fujimura and Tsuneta 2009, De Moortel and Nakariakov 2012). The three types of magnetohydrodynamic (MHD) waves are Alfvén, slow and fast modes; there are torsional, sausage and kink modes in magnetic flux tubes. The solar atmosphere is inhomogeneous, with the magnetic field concentrated at intergranular lanes in the photosphere, that fan out with height and merge in the transition region to the corona. In addition, there are strong magnetic fields in pores and sunspots (Bruzek and Durrant 1977, Athay and Holzer 1982). In the corona are observed spicules, loops and holes unrelated to the sunspots in the photosphere. Oscillations have been observed in all of these solar magnetic structures.

*Corresponding author. Email: andre.marta@tecnico.ulisboa.pt

The solar mass balance is established by spicules (Beckers 1968) that may be interpreted (Campos 1984) as slow modes or acoustic-gravity waves that become non-linear as they propagate upward in an atmosphere of decreasing density since the density profiles match; this agrees with the observation of oscillating upflows (De Pontieu *et al.* 2004, De Pontieu and McIntosh 2010, Tian, McIntosh and De Pontieu 2011) that have been interpreted as slow magnetoacoustic waves (Verwichte *et al.* 2010); in the corona, where the magnetic pressure exceeds the gas pressure, the acoustic-gravity waves follow magnetic field lines and spicules act as tracers of the solar magnetic field. The nonlinear acoustic-gravity waves grow into shocks, and their mass flux breaks out of the magnetic flux tube with a small part supplying the mass flux to the solar wind (Beckers 1972) and most of the rest causing downflows in the transition region (Pneumann and Kopp 1977, Engvold *et al.* 1985). There are numerous recent observations of longitudinal sausage, kink or higher modes (Ofman *et al.* 1997, DeForest and Gurman 1998, De Moortel *et al.* 2002, Srivastava *et al.* 2008, Yuan and Nakariakov 2012).

The observations of horizontal velocities in the low solar chromosphere (Beckers and Canfield 1975) can be interpreted as Alfvén-gravity waves (Ferraro and Plumpton 1958, Leroy 1980, Campos 1983) since they fit the growth of the amplitude of the velocity with altitude (Campos 1998). Alfvén or torsional modes are observed in the low solar chromosphere (Jess *et al.* 2009) and have for a long time been observed in the solar wind (Belcher and Davis 1971, Burlaga and Turner 1976, Campos 1998, Campos *et al.* 1999, Campos and Isaeva 2004). The observation of transversal motions in the corona (Aschwanden *et al.* 1999, De Pontieu *et al.* 2007, McIntosh *et al.* 2011, Tian, McIntosh, Habbal *et al.* 2011, Singh *et al.* 2011, Kuridze *et al.* 2012) have been given different interpretations either transversal torsional waves or longitudinal kink modes (Van Doorsselaere, Brady *et al.* 2008); as a result there is no consensus on the observation of Alfvén waves in the corona, although their observation both in the chromosphere and solar wind suggests they should also be present in the corona. The coupling of compressibility for longitudinal waves and transversal magnetic waves can lead for magneto-acoustic-gravity (MAG) waves to differential equations of the second (Nye and Thomas 1976, Adam 1977, Campos 1988), fourth (Campos 1985, Campos and Saldanha 1991) and sixth (Zhugzhda and Dzhalilov 1984) order. In contrast, Alfvén, slow and fast modes in magnetic flux tubes (Spruit 1981, 1982) are always decoupled and satisfy second-order differential equations due to the neglect of gravity.

The preceding references show two major influences on MHD waves in the solar atmosphere: (i) stratification in the sense of variation of the atmospheric properties with height; (ii) magnetic field structures, that is non-uniform magnetic fields. The present paper combines these two essential elements (i) and (ii) in the simplest possible way by considering one-dimensional magnetohydrostatic equilibrium (section 2) as the background state. This is consistent with zero divergence of a magnetic field varying with height, only it it is horizontal with fixed direction (section 2.1). This leads to a one-dimensional magnetohydrostatic equilibrium depending only on altitude for a perfect gas with arbitrary temperature profile and horizontal magnetic field with fixed direction and magnitude an arbitrary function of altitude (section 2.2). A particular case is an isothermal atmosphere under an horizontal magnetic field with fixed direction decaying with altitude on twice the scale height (section 2.3) leading to a constant sound speed and Alfvén speed decaying with altitude.

The MAG wave equation (section 3) is obtained for linear non-dissipative waves in a non-isothermal atmosphere under an arbitrary non-uniform magnetic field (section 3.1). In the case of vertical waves (i.e. that depend only on time and altitude, and an horizontal magnetic field with fixed direction and arbitrary dependence on altitude) the only possible mode is a magnetosonic-gravity wave with vertical velocity perturbation coupled to an horizontal

magnetic field perturbation parallel to the external magnetic field (section 3.2). In the case of an isothermal atmosphere under an horizontal magnetic field with fixed direction and decaying with altitude on twice the scale height, the exact solution of the magnetosonic-gravity wave equation is obtained in terms of confluent hypergeometric functions (section 3.3).

The preceding exact solution is applied to the solar atmosphere (section 4) for the typical conditions in the photosphere and transition region to the corona to demonstrate the effects of changes in mass density and magnetic field strength in these regions (section 4.1). These effects lead to a non-uniform propagation, and two consequences are: (i) whereas waves with constant propagation speed have sinusoidal waveforms with equally spaced nodes, a variable wave speed leads (section 4.2) to a deformation of the waveform with nodes more (less) spaced where the propagation speed increases (decreases) with altitude, as shown in figures 1–3; (ii) the deformation of the waveform affects the velocity and magnetic field gradients, and hence viscous and resistive heating, by dissipation of magnetosonic-gravity waves (section 4.3) that is not (is) sufficient to compensate the radiative losses of the chromosphere (corona) as shown in table 2.

The concluding discussion (section 5) distinguishes four kinds of theories of magneto-atmospheric waves : (i) those that neglect stratification and assume a uniform magnetic field as for ordinary MHD waves; (ii) current theories of wave modes in magnetic flux tubes neglect gravity and assume a magnetic field with different magnitude inside and outside, so that the magnetic field has an horizontal jump; (iii) theories of MAG waves that allow for the exponential decrease of density with height due to gravity in an isothermal atmosphere retaining hydrostatic equilibrium by assuming an uniform external magnetic field; (iv) theories combining atmospheric stratification due to gravity with non-uniform magnetic field in a background state of magnetohydrostatic equilibrium where MAG waves propagate. MAG The present theory of magneto-atmospheric waves is of type (iv) and thus the starting point is the simplest possible one-dimensional magnetohydrostatic equilibrium (section 2) that determines the wave speeds that appear as non-uniform coefficients in the wave equation.

2. Magnetohydrostatic equilibrium with horizontal magnetic field

A magnetohydrostatic equilibrium is considered for a non-isothermal atmosphere of a perfect gas under an horizontal magnetic field with fixed direction and arbitrary dependence on altitude (section 2.1). A particular case is an horizontal magnetic field decaying exponentially with altitude (section 2.2). The simplest case is an isothermal atmosphere, that is constant scale height, and horizontal magnetic field decaying exponentially with altitude on twice the scale height (section 2.3).

2.1. *Non-isothermal atmosphere under a non-uniform magnetic field*

In the case of a magnetic field $\boldsymbol{B}$ depending only on altitude z, the Maxwell equation

$$0 = \nabla \cdot [\boldsymbol{B}(z)] = \partial B_z / \partial z, \tag{1}$$

which states that $\boldsymbol{B}$ it has zero divergence, requires that the vertical component of the magnetic field be constant and allows the horizontal components to be arbitrary functions of altitude:

$$\boldsymbol{B}(z) = \boldsymbol{e}_z B_z + \boldsymbol{e}_x B_x(z) + \boldsymbol{e}_y B_y(z). \tag{2}$$

The magnetohydrostatic equilibrium of an atmosphere is specified by the balance of the gradient of the gas pressure against the weight and magnetic force:

$$\nabla p = \rho \boldsymbol{g} + \frac{\mu}{4\pi} (\nabla \times \boldsymbol{B}) \times \boldsymbol{B}, \tag{3}$$

where ρ is the mass density and $\boldsymbol{g}$ is the acceleration of gravity. The magnetic permeability μ is retained in the Lorentz force in (3) so that it applies for any choice of unit system. A uniform magnetic field would lead to zero Lorentz force and hydrostatic equilibrium. In order to have one-dimensional magnetohydrostatic equilibrium, the magnetic field must depend on altitude and can have only one non-zero horizontal component (4a):

$$\boldsymbol{B} = \boldsymbol{e}_x B(z)\,; \qquad \boldsymbol{g} = -\boldsymbol{e}_z g, \tag{4a,b}$$

the acceleration of gravity (4b) is assumed to be uniform and directed vertically downwards. The magnetic field (4a) implies an electrical current (5a) normal to the plane of gravity and the magnetic field, where prime denotes derivative with respect to altitude and c_0 is the speed of light in vacuum:

$$\boldsymbol{J} = \frac{c_0}{4\pi} \nabla \times \boldsymbol{B} = \boldsymbol{e}_y \frac{c_0}{4\pi} B'; \tag{5a}$$

$$\boldsymbol{F}m = \frac{\mu \boldsymbol{J} \times \boldsymbol{B}}{c_0} = -\boldsymbol{e}_z \frac{\mu B B'}{4\pi} = -\boldsymbol{e}_z P', \tag{5b}$$

the Lorentz force (5b) equals minus the vertical gradient of the magnetic pressure (6a):

$$P(z) = \frac{\mu}{8\pi} [B(z)]^2, \qquad (p + P)' = -\rho g, \tag{6a,b}$$

and thus magnetohydrostatic equilibrium (3) balances the weight against the vertical gradient of the total gas plus magnetic pressure (6b).

2.2. *Isothermal atmosphere and exponentially decaying magnetic field*

The equation of state for a perfect gas (7a), where T is the temperature and R is the gas constant, leads to (7b):

$$p = \rho R T, \qquad p' = -\frac{pg}{RT} - P'. \tag{7a,b}$$

In (7a,b) the temperature may vary with altitude and the scale height (8a) is specified by the temperature:

$$L(z) = \frac{R}{g} T(z), \qquad p' = -\frac{p}{L} - P', \tag{8a,b}$$

and applies only to the gas pressure (8b). In the case of a uniform magnetic field (9a) the hydrostatic equilibrium leads to the pressure (9b) valid for a non-isothermal atmosphere:

$$B = \text{const.}, \qquad p(z) = p(0) \exp\left[-\int_0^z \frac{\mathrm{d}\xi}{L(\xi)} \right]. \tag{9a,b}$$

In the presence of a non-uniform horizontal magnetic field (4a), the gas pressure is sought in the same form (9b) replacing the constant $p(0)$ by a function $Q(z)$:

$$p(z) = Q(z) \exp\left[-\int_0^z \frac{\mathrm{d}\xi}{L(\xi)} \right], \tag{10}$$

determined by substituting into (8b). That leads to

$$Q' \exp\left[-\int_0^z \frac{\mathrm{d}\xi}{L(\xi)}\right] = -P'; \tag{11a}$$

$$Q(z) = p(0) - \int_0^z P'(\eta)\left[\exp\int_0^\eta \frac{\mathrm{d}\xi}{L(\xi)}\right]\mathrm{d}\eta, \tag{11b}$$

the primitive of (11a) is (11b) and substituted in (10) specifies the gas pressure. The profile of the pressure as a function of altitude follows from (11b) and (10):

$$p(z) = p(0)\exp\left[-\int_0^z \frac{\mathrm{d}\xi}{L(\xi)}\right] - \exp\left[-\int_0^z \frac{\mathrm{d}\xi}{L(\xi)}\right]\int_0^z P'(\eta)\exp\left[\int_0^\eta \frac{\mathrm{d}\xi}{L(\xi)}\right]\mathrm{d}\eta, \tag{12}$$

for: (i) arbitrary temperature profile appearing in the scale height (8a); (ii) arbitrary profile of the strength of the magnetic field with fixed horizontal direction (4a) appearing in the magnetic pressure (6a).

The first term on the right-hand side of (12) corresponds to hydrostatic equilibrium (9b) under uniform magnetic field (9a), and the second term on the right-hand side of (12) is the effect of the non-uniform magnetic field.

The latter term may be integrated by parts:

$$\int_0^z P'(\eta)\exp\left[\int_0^\eta \frac{\mathrm{d}\xi}{L(\xi)}\right]\mathrm{d}\eta \tag{13}$$
$$= P(z)\exp\left[\int_0^z \frac{\mathrm{d}\xi}{L(\xi)}\right] - P(0) - \int_0^z \frac{P(\eta)}{L(\eta)}\exp\left[\int_0^\eta \frac{\mathrm{d}\xi}{L(\xi)}\right]\mathrm{d}\eta.$$

Substituting (13) into (12) leads to

$$p(z) + P(z) = [p(0) + P(0)]\exp\left[-\int_0^z \frac{\mathrm{d}\xi}{L(\xi)}\right] \tag{14}$$
$$+ \exp\left[-\int_0^z \frac{\mathrm{d}\xi}{L(\xi)}\right]\int_0^z \frac{P(\eta)}{L(\eta)}\exp\left[\int_0^\eta \frac{\mathrm{d}\xi}{L(\xi)}\right]\mathrm{d}\eta,$$

which specifies the total, gas plus magnetic, pressure profile.

The preceding expressions simplify for an isothermal atmosphere (15a) and magnetic field decaying exponentially with altitude (15b) on scale l:

$$T(z) = \text{const.} = T_0, \qquad B(z) = B_0 \mathrm{e}^{-z/l}, \tag{15a,b}$$

so that the magnetic pressure (6a) decays on half the scale from the value (16b) at altitude zero:

$$P(z) = P(0)\mathrm{e}^{-2z/l}, \qquad P(0) = \frac{\mu B_0^2}{8\pi}. \tag{16a,b}$$

Substitution of (15a) and (16a) into (12) leads to

$$p(z) - p(0)\mathrm{e}^{-z/L} = P(0)\frac{2}{l}\mathrm{e}^{-z/L}\int_0^z \mathrm{e}^{\eta(1/L-2/l)}\mathrm{d}\eta, \tag{17}$$

which specifies the profile of the gas pressure as a function of altitude:

$$l \neq 2L, \qquad p(z) = p(0)\mathrm{e}^{-z/L} + P(0)\frac{2L}{l-2L}\left(\mathrm{e}^{-2z/l} - \mathrm{e}^{-z/L}\right), \tag{18a,b}$$

which involves two length scales, namely: (i) the scale height (8a) for hydrostatic equilibrium (9b); (ii) the length scale $l/2$ for the magnetic pressure (16a). The profile of the gas pressure is given by (18b) when the two scales (i) and (ii) are unequal (18a). The case of coincidence of the two length scales is considered next.

2.3. *Horizontal magnetic field decaying on twice the scale height*

In the case of a magnetic field (15b) decaying with height on twice the scale height (8a), the second term on the right-hand side of (18b) may be evaluated as the limit:

$$\lim_{l\to 2L} \frac{2L}{l-2L} \mathrm{e}^{-z/L} \left[\mathrm{e}^{z(1/L-2/l)} - 1 \right] \tag{19}$$
$$= \lim_{l\to 2L} \mathrm{e}^{-z/L} \frac{2L}{l-2L} \left[(1/L - 2/l)\, z + \mathrm{O}\Big((1/L-2/l)^2 z^2 \Big) \right]$$
$$= \lim_{l\to 2L} \mathrm{e}^{-z/L} \left[2z/l + \mathrm{O}\left(\frac{l-2L}{Ll^2} z^2 \right) \right] = \frac{z}{L} \mathrm{e}^{-z/L}.$$

Substituting (19) into (18b) leads to the profile of the gas pressure (20b) in the case of coincident length scales (20a):

$$l = 2L \; : \qquad p(z) = \left[p(0) + P(0) \frac{z}{L} \right] \mathrm{e}^{-z/L}. \tag{20a,b}$$

This result can be checked by using (20a) in the magnetic field (15b) and pressure (16a) leading, respectively, to (21a,b):

$$B(z) = B_0 \mathrm{e}^{-z/(2L)}, \quad P(z) = -P(0) \mathrm{e}^{-z/L}, \quad p' = -\frac{p}{L} + \frac{P(0)}{L} \mathrm{e}^{-z/L}, \tag{21a–c}$$

and (7b) to the magnetohydrostatic equilibrium condition (21c). Seeking a gas pressure profile of the form (22a) leads by substitution in (21c)–(22b):

$$p(z) = Q(z) \mathrm{e}^{-z/L}, \quad Q'(z) = \frac{P(0)}{L}; \quad Q(z) = p(0) + P(0) \frac{z}{L}. \tag{22a–c}$$

The primitive of (22b) is (22c), which upon substitution into (22a) confirms (20b).

The sound speed c is constant for an isothermal atmosphere (23a), where γ is the adiabatic index:

$$c^2 = \gamma \frac{p_0}{\rho_0} = \gamma R T_0; \qquad a^2 = \frac{\mu B_0^2}{4\pi \rho_0} = \frac{2P_0}{\rho_0}, \tag{23a,b}$$

the Alfvén speed at an altitude $z = 0$ is given by (23b), and their ratio squared specifies (24a) the wave speed parameter

$$\varepsilon \equiv \frac{a^2}{c^2} = \frac{2P_0}{\gamma \rho_0} = \frac{2}{\gamma \beta}, \qquad \beta \equiv \frac{p_0}{P_0} = \frac{p(0)}{P(0)}, \tag{24a,b}$$

which is related to the plasma-β defined (24b) as the ratio of gas to magnetic pressures at altitude zero. The latter appears in the profiles of gas pressure and mass density:

$$\frac{p(z)}{p_0} = \frac{\rho(z)}{\rho_0} = \left(1 + \frac{z}{\beta L} \right) \mathrm{e}^{-z/L}, \tag{25a,b}$$

which are the same for a perfect gas (7a) in an isothermal atmosphere (15a). The profile of the gas pressure (25a) is distinct from that of the magnetic pressure (21b), and thus although the sound speed is constant (23a), the Alfvén speed (26a) is not:

$$[A(z)]^2 = \frac{\mu [B(z)]^2}{4\pi \rho(z)} = \frac{\mu B_0^2}{4\pi \rho_0} \frac{1}{1 + z/\beta L} = \frac{a^2}{1 + z/\beta L}, \tag{26a,b}$$

and decays with altitude (26b). The coefficients in the MAG wave equation involve the inverse length scales (27a,b) respectively of the magnetic field (21a) and mass density (25b):

$$\frac{B'(z)}{B(z)} = -\frac{1}{2L}, \qquad \frac{\rho'(z)}{\rho(z)} = -\frac{1}{L} + \frac{1}{z+\beta L}, \tag{27a,b}$$

besides the sound (23a) and Alfvén (26b), (23b) speeds.

3. Magnetosonic-gravity waves in a non-uniform magnetic field

Our starting point is the linear MAG wave equation for a non-isothermal atmosphere under a non-uniform magnetic field (section 3.1). In the particular case of an horizontal external magnetic field, the MAG waves reduce to magnetosonic-gravity wave mode described by a second-order differential equation, instead of differential systems of orders 4 or 6 for general MAG waves in an oblique external magnetic field. In the case section 2.3 of an isothermal atmosphere under an horizontal magnetic field with fixed direction and strength decaying exponentially with altitude on twice the scale height for vertical waves depending only on altitude and time: (i) the horizontal components of the velocity perturbation are conserved; (ii) only the vertical velocity propagates corresponding to magnetosonic-gravity waves (section 3.2). The exact solution of the vertical magnetosonic-gravity wave equation is obtained in terms of confluent hypergeometric functions (section 3.3).

3.1. *MAG wave equation with non-uniform temperature and magnetic field*

The fundamental equations of non-dissipative MHDs in the presence of a gravity field are: (i) the magnetic induction equation

$$\frac{\partial \boldsymbol{H}}{\partial t} + \boldsymbol{\nabla} \times (\boldsymbol{H} \times \boldsymbol{V}) = \boldsymbol{0}, \tag{28}$$

where $\boldsymbol{V}$ is the velocity and $\boldsymbol{H}$ the total (background $\boldsymbol{B}$ plus perturbation $\boldsymbol{h}$) magnetic field; (ii) the equation of continuity

$$\frac{\partial \Gamma}{\partial t} + \boldsymbol{\nabla} \cdot (\Gamma \boldsymbol{V}) = \boldsymbol{0}, \tag{29}$$

where Γ is total the mass density; (iii) the momentum equation

$$\Gamma \left[\frac{\partial \boldsymbol{V}}{\partial t} + (\boldsymbol{V} \cdot \boldsymbol{\nabla}) \boldsymbol{V} \right] + \boldsymbol{\nabla} \overline{p} = \Gamma \boldsymbol{g} - (\mu/4\pi) \boldsymbol{H} \times (\boldsymbol{\nabla} \times \boldsymbol{H}), \tag{30}$$

where $\overline{p}$ is the total gas pressure and $\boldsymbol{g}$ the acceleration of gravity; (iv) the adiabatic equation

$$\frac{\partial \overline{p}}{\partial t} + \boldsymbol{V} \cdot \boldsymbol{\nabla} \overline{p} = c^2 \left(\frac{\partial \Gamma}{\partial t} + \boldsymbol{V} \cdot \boldsymbol{\nabla} \Gamma \right), \tag{31}$$

where c is the adiabatic sound speed. The total state of the fluid is assumed to consist of an inhomogeneous mean state of rest upon which are superimposed unsteady non-uniform perturbations:

$$\begin{aligned} \boldsymbol{H}(\boldsymbol{x}, t) &= \boldsymbol{B}(\boldsymbol{x}) + \boldsymbol{h}(\boldsymbol{x}, t), & \boldsymbol{V}(\boldsymbol{x}, t) &= \boldsymbol{0} + \boldsymbol{v}(\boldsymbol{x}, t), \\ \Gamma(\boldsymbol{x}, t) &= \rho(\boldsymbol{x}) + \rho'(\boldsymbol{x}, t), & \overline{p}(\boldsymbol{x}, t) &= p(\boldsymbol{x}) + p'(\boldsymbol{x}, t). \end{aligned} \tag{32}$$

The MAG wave equation is obtained (Campos 1987) by linearisation followed by elimination for the velocity.

Substituting of (32a–d), subtracting the mean state and linearising leads from (28)–(31) to

$$\frac{\partial \boldsymbol{h}}{\partial t} + \nabla \times (\boldsymbol{B} \times \boldsymbol{v}) = \boldsymbol{0}, \tag{33a}$$

$$\frac{\partial \rho'}{\partial t} + \boldsymbol{v} \cdot \nabla \rho + \rho \, (\nabla \cdot \boldsymbol{v}) = 0, \tag{33b}$$

$$\rho \frac{\partial \boldsymbol{v}}{\partial t} + \nabla p' = \rho' \boldsymbol{g} - (\mu/4\pi) \, [\boldsymbol{B} \times (\nabla \times \boldsymbol{h}) + \boldsymbol{h} \times (\nabla \times \boldsymbol{B})] \, , \tag{33c}$$

$$\frac{\partial p'}{\partial t} + \boldsymbol{v} \cdot \nabla p = c^2 \left(\frac{\partial \rho'}{\partial t} + \boldsymbol{v} \cdot \nabla \rho \right) . \tag{33d}$$

Substituting (33b) on the right-hand side of (33d) and (3) on the left-hand side leads to

$$\frac{\partial p'}{\partial t} = -\rho c^2 \, (\nabla \cdot \boldsymbol{v}) - \rho \boldsymbol{v} \cdot \boldsymbol{g} - \frac{\mu}{4\pi} \boldsymbol{v} \cdot [(\nabla \times \boldsymbol{B}) \times \boldsymbol{B}] \, . \tag{34}$$

Applying $\partial / \partial t$ to (33c) and substituting (33a), (33b), (34) leads to the linear non-dissipative MAG wave equation

$$\begin{aligned} \rho \frac{\partial^2 \boldsymbol{v}}{\partial t^2} - \nabla \left\{ \rho c^2 \, (\nabla \cdot \boldsymbol{v}) + \rho \boldsymbol{v} \cdot \boldsymbol{g} + \frac{\mu}{4\pi} \boldsymbol{v} \cdot [(\nabla \times \boldsymbol{B}) \times \boldsymbol{B}] \right\} \\ = -\boldsymbol{g} \, [\nabla \cdot (\rho \boldsymbol{v})] + \frac{\mu}{4\pi} \boldsymbol{B} \times \{ \nabla \times [\nabla \times (\boldsymbol{B} \times \boldsymbol{v})] \} \\ + \frac{\mu}{4\pi} \, [\nabla \times (\boldsymbol{B} \times \boldsymbol{v})] \times (\nabla \times \boldsymbol{B}) \, , \end{aligned} \tag{35}$$

with the velocity perturbation as variable:

$$\begin{aligned} \rho \frac{\partial^2 \boldsymbol{v}}{\partial t^2} - \nabla \left[\rho c^2 \, (\nabla \cdot \boldsymbol{v}) \right] - \nabla \, [\rho \, (\boldsymbol{v} \cdot \boldsymbol{g})] + \boldsymbol{g} \, [\nabla \cdot (\rho \boldsymbol{v})] \\ = \frac{\mu}{4\pi} \boldsymbol{B} \times \{ \nabla \times [\nabla \times (\boldsymbol{B} \times \boldsymbol{v})] \} + \frac{\mu}{4\pi} \, [\nabla \times (\boldsymbol{B} \times \boldsymbol{v})] \times (\nabla \times \boldsymbol{B}) \\ + \nabla \left\{ \frac{\mu}{4\pi} \boldsymbol{v} \cdot [(\nabla \times \boldsymbol{B}) \times \boldsymbol{B}] \right\} , \end{aligned} \tag{36}$$

valid for a non-isothermal atmosphere under non-uniform gravity and magnetic fields. The seven terms in the linear non-dissipative MAG wave equation (36) are interpreted as follows from left to right: (i) second-order time dependence allowing propagation in opposite directions and superposition into standing waves; (ii) acoustic propagation involving the sound speed c and dilatation $\nabla \cdot \boldsymbol{v}$; (iii) gravity waves involving the acceleration of gravity $\boldsymbol{g}$; (iv) acoustic-gravity coupling through ρ, $\boldsymbol{g}$ and $\nabla \cdot \boldsymbol{v}$; (v) hydromagnetic waves for uniform magnetic field; (vi)–(vii) the case of non-uniform magnetic field adds the last two terms. The MAG wave equation (36) simplifies in the case of an isothermal atmosphere (37a) and uniform magnetic field (37b)–(37c):

$$c = \text{const.}, \qquad \boldsymbol{B} = \text{const.} : \tag{37a,b}$$

$$\frac{\partial^2 \boldsymbol{v}}{\partial t^2} - c^2 \nabla \, (\nabla \cdot \boldsymbol{v}) - \nabla \, (\boldsymbol{v} \cdot \boldsymbol{g}) - (\gamma - 1) \, \boldsymbol{g} \, (\nabla \cdot \boldsymbol{v}) + \frac{\mu}{4\pi\rho} \boldsymbol{B} \times \{ \nabla \times [\nabla \times (\boldsymbol{B} \times \boldsymbol{v})] \} = \boldsymbol{0}, \tag{37c}$$

which is well known (McLellan and Winterberg 1968, Bray and Loughhead 1974). In the passage from (36) to (37c) we have used

$$-\frac{1}{\rho}\nabla\left[\rho c^2\left(\nabla\cdot\boldsymbol{v}\right)\right]-\frac{1}{\rho}\nabla\left[\rho\left(\boldsymbol{v}\cdot\boldsymbol{g}\right)\right]+\frac{\boldsymbol{g}}{\rho}\left[\nabla\cdot\left(\rho\boldsymbol{v}\right)\right]$$
$$=-c^2\nabla\left(\nabla\cdot\boldsymbol{v}\right)-\nabla\left(\boldsymbol{v}\cdot\boldsymbol{g}\right)+\left(\nabla\cdot\boldsymbol{v}\right)\left[\boldsymbol{g}-\frac{\nabla\left(\rho c^2\right)}{\rho}\right]-\left(\boldsymbol{v}\cdot\boldsymbol{g}\right)\frac{\nabla\rho}{\rho}+\frac{\boldsymbol{g}}{\rho}\left(\boldsymbol{v}\cdot\nabla\rho\right), \tag{37}$$

where: (i) the first two terms appear in (37c); (ii) using the sound speed and condition of hydrostatic equilibrium, the next two terms combine as

$$\boldsymbol{g}-\frac{\nabla\left(\rho c^2\right)}{\rho}=\boldsymbol{g}-\frac{\nabla\left(\gamma p\right)}{\rho}=\boldsymbol{g}\left(1-\gamma\right), \tag{37e}$$

which also appears in (37c); (iii) the last two terms in (37d) cancel because $\boldsymbol{g}$ and $\nabla\rho$ are both vertical downward and hence parallel. In the absence of gravity, (37c) is the MHD wave equations (Herlofson 1950, Alfvén and Falthammar 1962, Campos 1977) in an homogeneous isothermal medium under a uniform magnetic field.

Next we consider the case of a non-uniform horizontal magnetic field with fixed direction (38a):

$$\boldsymbol{B}(\boldsymbol{x})=\boldsymbol{e}_x B(z)\,,\qquad \boldsymbol{v}(\boldsymbol{x},t)=\boldsymbol{e}_x v_x(z,t)+\boldsymbol{e}_y v_y(z,t)+\boldsymbol{e}_z v_z(z,t), \tag{38}$$

for vertical waves (38b) depending only on altitude and time. Denoting by dot time derivative (39a) and prime the derivative with regard to altitude (39b), it follows from (36) that both horizontal components of the velocity perturbation are conserved (39c,d):

$$\dot{f}\equiv\partial f/\partial t,\qquad f'\equiv\partial f/\partial z:\qquad\qquad \ddot{v}_x=0,\qquad \ddot{v}_y=0, \tag{39}$$

because: (i) in both cases the horizontal gradients in the second and third terms on the left-hand side of (36) are zero and there is no acoustic propagation; (ii) in the fourth term on the left-hand side of (36) there is no gravity effect (4b) in the horizontal direction; (iii) the horizontal velocity is orthogonal to the vertical external magnetic force (5b) in the last term of the right-hand side of (36); (iv) the external magnetic field in the x-direction (38a) does not act on the velocity perturbation v_x in the same direction in the first two terms on the right-hand side of (36); (v) the preceding (i) to (iv) confirm (39c); (vi) concerning (39d) the same arguments (i) to (iii) apply except (iv); (vii) concerning the first two terms on the right-hand side of (36) they cancel for the velocity perturbation v_y out of the plane of gravity $\boldsymbol{g}$ and the external magnetic field $\boldsymbol{B}$ because it would correspond to Alfvén waves propagating along the horizontal magnetic field, but horizontal propagation is excluded by (38b); (viii) this confirms (39d).

3.2. *Vertical magnetosonic-gravity waves*

Thus only vertical velocity perturbation can propagate vertically and it satisfies (36), the magnetosonic-gravity wave equation

$$\rho\ddot{v}_z-\left(\rho c^2 v_z'\right)'+\left(\rho g v_z\right)'-g\left(\rho v_z\right)'=\frac{\mu}{4\pi}\left[B\left(Bv_z\right)''+B'\left(Bv_z\right)'-\left(B'Bv_z\right)'\right]. \tag{40}$$

The last two terms on the left-hand side of (40) cancel for a uniform gravity field (41a) and the remaining terms simplify to (41b):

$$g = \text{const.}: \qquad \ddot{v}_z - \left(c^2 v_z'\right)' - c^2 \frac{\rho'}{\rho} v_z' = \frac{\mu}{4\pi\rho}\left(B^2 v_z'' + 2B'B v_z'\right). \tag{41a,b}$$

Since the atmospheric mean state does not depend on time, the vertical velocity perturbation may be expressed as the Fourier integral

$$v_z(z,t) = \int_{-\infty}^{+\infty} V(z;\omega) \mathrm{e}^{-\mathrm{i}\omega t} \mathrm{d}\omega, \tag{42}$$

where the vertical velocity spectrum for a wave of frequency ω at altitude z satisfies

$$\left(c^2 + A^2\right) V'' + \left(c^2 \frac{\rho'}{\rho} + 2c'c + 2A^2 \frac{B'}{B}\right) V' + \omega^2 V = 0, \tag{43}$$

using the Alfvén speed (26a). In an isothermal atmosphere, the sound speed is constant (44a), and for a uniform magnetic field (44b) the mass density decays on the scale height (44c):

$$c = \text{const.}, \qquad B = \text{const.}: \qquad \frac{\rho'}{\rho} = -\frac{1}{L} = -\frac{g}{RT} = -\frac{\gamma g}{c^2}; \tag{44a–c}$$

in this case the magnetosonic-gravity wave equation for vertically propagating waves in a isothermal atmosphere under an uniform horizontal magnetic field reduces to

$$\left(c^2 + A^2\right) V'' - \gamma g V' + \omega^2 V = 0, \tag{44d}$$

whose exact solution can be obtained in terms of Gaussian hypergeometric functions (Campos 1983, Campos 1985); the extension to horizontal propagation has also been considered (Nye and Thomas 1976, Adam 1977, Campos 1988). In the absence of magnetic field, omission of the Alfvén speed leads to the acoustic-gravity wave equation (Campos 1983, Pedlosky 1990).

In an isothermal atmosphere with horizontal magnetic field decaying exponentially with altitude on twice the scale height (27a), the magnetosonic-gravity wave equation (43) becomes

$$\left(c^2 + A^2\right) V'' - \left(\frac{c^2}{L} - \frac{c^2}{z + \beta L} + \frac{A^2}{L}\right) V' + \omega^2 V = 0, \tag{45a}$$

using (27b). Substituting the Alfvén speed (26b) leads to

$$\left(1 + \frac{2L/\gamma}{z + \beta L}\right) V'' - \left(\frac{1}{L} - \frac{1 - 2/\gamma}{z + \beta L}\right) V' + \frac{\omega^2}{c^2} V = 0, \tag{45b}$$

where (24a) was used:

$$\frac{a^2}{c^2}\beta = \beta\varepsilon = \frac{2}{\gamma}: \qquad \frac{A^2}{L} = \frac{c^2\varepsilon}{L + z/\beta} = \frac{c^2\varepsilon\beta}{z + \beta L} = \frac{2c^2/\gamma}{z + \beta L}, \tag{46}$$

involving the parameter ε that is related to the plasma-β the ratio of gas and magnetic pressures (24b) at altitude zero. Introducing the dimensionless altitude (47a) and frequency (47b) using the scale height :

$$\zeta \equiv \frac{z}{L}, \qquad \Omega \equiv \frac{\omega L}{c}: \qquad V(z;\omega) = U(\zeta;\Omega,\gamma,\beta), \tag{47}$$

the vertical velocity perturbation (47c) satisfies a linear second-order differential equation with variable coefficients:

$$\left(1 + \frac{2/\gamma}{\zeta + \beta}\right) U'' - \left(1 - \frac{1 - 2/\gamma}{\zeta + \beta}\right) U' + \Omega^2 U = 0, \tag{48a}$$

involving three dimensionless parameters: (i) the Helmholtz number or frequency made dimensionless using the sound speed and scale height (47b); (ii) the plasma-β or ratio of gas to magnetic pressure at zero altitude (24b); (iii) the parameter (24a) that is the ratio of Alfvén to sound speed squared at zero altitude that is related to the plasma-β through the adiabatic index γ in the sound speed (23a). The differential equation (48a) is linear of second-order with coefficients that are linear functions of the independent variable ζ and hence is reducible (Kamke 1944) to the confluent hypergeometric type.

The differential equation (48a) for magnetosonic-gravity waves, in the form

$$(\beta + 2/\gamma + \zeta)\, U'' + (1 - \beta - 2/\gamma - \zeta)\, U' + \Omega^2(\beta + \zeta)U = 0, \tag{48b}$$

is reducible to the confluent hypergeometric type (Erdélyi 1953) with parameters (b, d) and variable η that can take any real or complex values:

$$\eta T'' + (f - \eta)T' - bT = 0, \tag{49}$$

via three changes of variable with a clear physical interpretation. The first change uses the coefficient of U'' in (48a) as a new independent variable (50a):

$$\xi = \beta + 2/\gamma + \zeta, \qquad U(\zeta, \Omega, \gamma, \beta) = G(\xi), \tag{50a,b}$$

leading (50b) to the differential equation (51):

$$\xi G'' + (1 - \xi)\, G' + \Omega^2\, (\xi - 2/\gamma)\, G = 0; \tag{51}$$

the first terms of (49) and (51) coincide. The physical interpretation is that the independent variable (50a) vanishes (52a) at the critical layer or singularity corresponding to the altitude (52a,b):

$$\xi_c = 0: \qquad \frac{z_c}{L} = -\beta - \frac{2}{\gamma} = -\frac{2}{\gamma}\left(1 + \frac{1}{\varepsilon}\right) = -\frac{2}{\gamma}\left(1 + \frac{c^2}{a^2}\right), \tag{52a,b}$$

where was used (24b) the plasma-β and (24a) the ratio of the squares of the Alfvén and sound speeds at altitude $z = 0$. Bearing in mind that the sound speed is constant (23a) in an isothermal atmosphere and the Alfvén speed (26a) decays with altitude (26b) for the non-uniform external magnetic field (21a), it follows that: (i) far below the critical level $z \ll z_c$, the Alfvén speed predominates and the waves are mainly hydromagnetic-gravity waves modified by compressibility; (ii) far above the critical layer $z \gg z_c$, the sound speed predominates and the waves are mainly acoustic-gravity waves modified by the magnetic field; (iii) across the critical layer $z \sim z_c$, the magnetosonic-gravity waves are converted gradually between predominantly hydromagnetic below and acoustic above.

3.3. *Exact solutions in terms of confluent hypergeometric functions*

The differential equation (51) differs from the confluent hypergeometric type (49) mainly in that the variable ξ appears in the coefficient of G. This may be dealt with via a change of dependent variable (53a) leading to (53b):

$$G(\xi) = \mathrm{e}^{\vartheta\xi} S(\xi): \tag{53a}$$

$$\xi S'' + [1 - (1 - 2\vartheta)\,\xi]\, S' + \left[\left(\vartheta^2 - \vartheta + \Omega^2\right)\xi + \vartheta - 2\Omega^2/\gamma\right] S = 0, \tag{53b}$$

where the constant ϑ can be chosen at will. It is chosen to be the root of (54a) so as to cancel the coefficient ξS in (53b) leading to (54b):

$$\vartheta^2 - \vartheta + \Omega^2 = 0 : \tag{54a}$$

$$\xi S'' + [1 - (1 - 2\vartheta)\,\xi]\,S' + \left(\vartheta - 2\Omega^2/\gamma\right) S = 0. \tag{54b}$$

The roots of (54a) are given by

$$2\vartheta_\pm = 1 \pm \sqrt{1 - 4\Omega^2} = 1 \pm \mathrm{i}\kappa, \qquad \kappa \equiv \sqrt{4\Omega^2 - 1}; \tag{55a,b}$$

substituting (55a) in the exponential factor in (53a) and using (50a), (47a) gives

$$\begin{aligned}\exp(\vartheta\xi) &= \exp\left[\frac{1 \pm \mathrm{i}\kappa}{2}\left(\beta + \frac{2}{\gamma} + \frac{z}{L}\right)\right] \\ &= \exp\left[\frac{1 \pm \mathrm{i}\kappa}{2}\left(\beta + \frac{\gamma}{2}\right)\right]\exp\left(\frac{z}{2L} \pm \mathrm{i}\kappa\frac{z}{2L}\right).\end{aligned} \tag{56}$$

The first factor in (56) is a constant of no interest and the second gives the physical interpretation of the change of dependent variable (53a), namely: (i) $\exp(z/2L) \sim 1/\sqrt{\rho(z)}$ specifies the increase of amplitude with altitude for acoustic-gravity waves in an isothermal atmosphere; (ii) the role of effective vertical wavenumber in (56) is played by

$$k \equiv \frac{\kappa}{2L} = \frac{1}{2L}\sqrt{\frac{4\omega^2L^2}{c^2} - 1} = \frac{\omega}{c}\sqrt{1 - \frac{c^2}{4\omega^2L^2}} = \frac{\omega}{c}\sqrt{1 - \left(\frac{\omega_*}{\omega}\right)^2}, \tag{57a}$$

where

$$\omega_* = \frac{c}{2L} \tag{57b}$$

is the cut-off frequency; (iii) above the cut-off frequency $\omega > \omega_*$, the effective vertical wavenumber is real, corresponding to propagating waves, and below $\omega < \omega_*$, it is imaginary, corresponding to evanescent modes. Thus the factor (56) in (53a) corresponds to acoustic-gravity waves that dominate the magnetosonic-gravity wave field at high-altitude when the Alfvén speed (26b) speed is small compared with the sound speed (23a). The solution of (53b) specifies the effect of the magnetic field that is important at lower altitudes, closer to and below the critical level (52b).

Substituting (55a) into (53b) leads to the differential equation

$$\xi S'' + (1 \pm \mathrm{i}\kappa\xi)\,S' + \left(\frac{1 \pm \mathrm{i}\kappa}{2} - \frac{2\Omega^2}{\gamma}\right) S = 0, \tag{58}$$

which reduces to the confluent hypergeometric type (49) via a third and final change of variable that is the simple re-scaling

$$\eta \equiv \mp\mathrm{i}\kappa\xi, \qquad S(\xi) = T(\eta). \tag{59a,b}$$

The change of independent variable (59a) leads from (58) and (59b) to the differential equation

$$\eta T'' + (1 - \eta)T' - \left(\frac{1}{2} \pm \frac{1}{2\mathrm{i}\kappa} \mp \frac{2\Omega^2}{\mathrm{i}\kappa\gamma}\right) T = 0. \tag{60}$$

The latter is of the confluent hypergeometric type (49) with parameter (b, f) where $f = 1$ and b is given by (61b) using (55b) (equivalent to (61a)):

$$4\Omega^2 = 1 + \kappa^2 : \qquad b = \frac{1}{2} \pm \frac{1}{2\mathrm{i}\kappa} \mp \frac{1 + \kappa^2}{2\mathrm{i}\kappa\gamma} = \frac{1}{2} \mp \frac{\mathrm{i}}{2\kappa} \pm \frac{\mathrm{i}}{2\kappa\gamma} \pm \frac{\mathrm{i}\kappa}{2\gamma}. \tag{61a,b}$$

One solution of the confluent hypergeometric equation (49) with second parameter $f = 1$ is a function of the first kind (Campos 2012):

$$\mathrm{F}(b; 1; \eta) = 1 + \sum_{n=0}^{\infty} \frac{\eta^n}{n!} b(b+1)...(b+n-1), \tag{62}$$

which is unity for $\eta_c = 0$, corresponding (59a) to the critical layer (52a,b). The choice of two signs in (55a) leads to two linearly independent solutions of the wave equation specified by confluent hypergeometric functions of the first kind (62) leading through (59a,b), (53a), (56), (50a,b), (47a,c) to the vertical velocity perturbation spectrum

$$V_{\pm}(z; \omega) = \mathrm{e}^{z/2L} \mathrm{e}^{\pm \mathrm{i}kz} \mathrm{F}\left(\frac{1}{2} \mp \frac{\mathrm{i}}{2\kappa} \pm \frac{\mathrm{i}}{2\kappa\gamma} \pm \frac{\mathrm{i}\kappa}{2\gamma};\ 1;\ \mp \mathrm{i}\kappa \left(\beta + \frac{2}{\gamma} + \frac{z}{L} \right) \right), \tag{63}$$

where: (i) the exponential factors (56) correspond to upward V_+ and downward V_- propagating acoustic-gravity waves that dominate asymptotically at high-altitude; (ii) the confluent hypergeometric function accounts for the effects of the magnetic field that are more significant close to or below the critical layer (52a,b). The general wave field is a linear combination of both, with arbitrary amplitudes $A_{\pm}$:

$$V(z; \omega) = A_+ V_+(z; \omega) + A_- V_-(z; \omega). \tag{64}$$

Since $V_{\pm}$ are complex conjugates (65a), a standing wave field (65c) is obtained for real equal amplitudes (65b):

$$V_-^*(z; \omega) = V_+(z; \omega), \qquad A_+ = A_- \equiv A, \qquad V(z; \omega) = 2A\, \mathrm{Re}\{V_{\pm}(z; \omega)\}. \tag{65a–c}$$

Since the confluent hypergeometric equation (60) (eqivalent to (49)) has parameters $(b, 1)$ besides the confluent hypergeometric function of the first kind (62), another linearly independent solution is a confluent hypergeometric function of the second kind (appendix A). Each of the confluent hypergeometric functions of the first and second kinds leads to two solutions of the wave equation (45b) choosing $\pm$ sign in (56), leading to a total of four solutions. All four solutions have comparable asymptotic scaling at low $z \to -\infty$ and high $z \to +\infty$ altitude (appendix B). The main difference is that (a) the confluent hypergeometric functions of the first kind are finite everywhere and those (b) of second kind are singular at the critical layer. The general integral can be chosen as a linear combination of any two of the four solutions. The solutions finite everywhere are chosen for application to the solar atmosphere.

4. Oscillations in the solar corona and heating of the transition region

The application of the preceding theory of magnetosonic-gravity waves (section 3) in a non-uniform magnetic field (section 2) to the solar atmosphere (section 4) specifies the values of physical parameters (section 4.1) that: (i) demonstrate the decreasing spacing nodes (figures 1–3) due to the decrease of Alfvén speed with altitude (section 4.2); (ii) the large waveform

gradients and intense dissipation in the transition region (section 4.3) that leads by evaporation to high coronal temperatures.

4.1. *Physical parameters in the solar atmosphere*

Table 1 summarises solar data (Athay 1976, Bruzek and Durrant 1977) relevant to the present problem of magneto-atmospheric waves. The temperature varies from $T_1 = 6.4 \times 10^3$ K in the photosphere through a minimum in the chromosphere to a maximum of $T_2 = 1.8 \times 10^6$ K in the corona. The mass density decays from $\rho_1 = 3.0 \times 10^{-7}$ g cm^{-3} in the photosphere to $\rho_2 = 1.3 \times 10^{-13}$ g cm^{-3} in the corona. The intense magnetic field $B_1 = 1.5 \times 10^3$ G is concentrated in flux tubes at intergranular lanes in the photosphere that fan out with altitude leading to the average solar magnetic field $B_2 = 20$ G in the corona. The temperature, mass density and external magnetic field specify all the atmospheric parameters needed to describe the propagation of MAG waves using the gas constant $R = 8.3 \times 10^7$ g cm^2 s^{-2} K^{-1} mol^{-1}. Considering non-ionised diatomic hydrogen with adiabatic index $\gamma_1 = 7/5$ at the photosphere leads to (23a) the sound speed $c_1 = \sqrt{\gamma_1 R T_1} = 8.6 \times 10^5$ cm s^{-1}; the adiabatic index $\gamma_2 = 5/3$ for fully ionised monatomic hydrogen at the coronal temperature T_2 leads to a much larger sound speed $c_2 = \sqrt{\gamma_2 R T_2} = 1.6 \times 10^7$ cm s^{-1}. The Alfvén speed (23b) at granulation boundaries in the photosphere $a_1 = B_1\sqrt{\mu/4\pi\rho_1} = 7.7 \times 10^5$ cm s^{-1} is comparable to the sound speed, though much smaller elsewhere; in the corona, the Alfvén speed $a_2 = B_2\sqrt{\mu/4\pi\rho_2} = 1.6 \times 10^7$ cm s^{-1} is again comparable to the sound speed. Thus parameter (24a) does not vary too much between $\varepsilon_1 = (a_1/c_1)^2 = 0.8$ at the granulation boundaries in the photosphere and $\varepsilon_2 = (a_2/c_2)^2 = 1.0$ in the corona, as the magnetic flux tubes expand from 1.5% of the solar surface to the whole solar disk. The corresponding plasma-β or (24b) ratios of gas to magnetic pressure are $\beta_1 = 2/(\gamma_1\varepsilon_1) = 1.8$ at the granulation boundaries in the photosphere and much smaller elsewhere compared to $\beta_2 = 2/(\gamma_2\varepsilon_2) = 1.2$ in the corona. All these values are orders of magnitude since the solar photosphere, chromosphere, corona and transition region have properties varying with altitude, most rapidly in the last named (transition region).

The decay of the magnetic field with altitude from granulation boundaries in the photosphere to the corona $B_1/B_2 = 1.5 \times 10^3/20 = 75$ is smaller than the decay of the square root of mass density $\sqrt{\rho_1/\rho_2} = \sqrt{3.0 \times 10^{-7}/1.3 \times 10^{-13}} = 1.5 \times 10^3$ and the increase in temperature $T_2/T_1 = 1.8 \times 10^6/6.4 \times 10^3 = 2.8 \times 10^2$ is intermediate. Besides the sound (23a) and Alfvén (23b) speeds, the scale height (8a) and cut-off frequency (57b):

$$\omega_* = \frac{c}{2L} = \frac{\sqrt{\gamma RT}}{2RT/g} = \frac{g}{2}\sqrt{\frac{\gamma}{RT}}, \tag{66}$$

also vary with altitude. Using the solar gravity $g = 2.7 \times 10^4$ cm s^{-2}, the scale height varies from a minimum $L_1 = RT_1/g = 2.0 \times 10^7$ cm in the chromosphere to a much larger value $L_2 = RT_2/g = 5.5 \times 10^9$ cm in the corona. The cut-off frequency decreases from $\omega_1^* = (g/2)\sqrt{\gamma_1/RT_1} = 2.2 \times 10^{-2}$ s^{-1} to $\omega_2^* = (g/2)\sqrt{\gamma_2/RT_2} = 1.4 \times 10^{-3}$ s^{-1}, corresponding to an increase in the cut-off period from $\tau_1^* = 2\pi/\omega_1^* = 2.9 \times 10^2$ s to $\tau_2^* = 2\pi/\omega_2^* = 4.4 \times 10^3$ s. Since the propagation is possible above the cut-off frequency,, that is below the cut-off period, the most restrictive value is close to the 5 min oscillation $\tau = 3.0 \times 10^2$ s, suggesting that higher frequency waves are strongly attenuated by dissipation, leading to atmospheric heating (section 4.3). The 5 min oscillation $\tau = 3.0 \times 10^2$ s corresponds to the frequency $\omega = 2\pi/\tau = 2.1 \times 10^{-2}$ s, and to the dimensionless frequency (47b) or

Table 1. Physical conditions in the solar atmosphere.

Physical quantity	Symbol	Equation	Photosphere	Corona	Unit
Temperature	T	–	6.4×10^3	1.8×10^6	K
Mass density	ρ	–	3.0×10^{-7}	1.3×10^{-13}	g cm^{-3}
Magnetic field	B	–	1.5×10^3	2.0×10	G
Adiabatic index	γ	(70a,b)	1.4	1.67	–
Scale height	L	(8a)	2.0×10^7	5.5×10^9	cm
Sound speed	c	(23a)	8.6×10^5	1.6×10^7	cm s^{-1}
Alfvén speed	a	(26a)	7.7×10^5	1.6×10^7	cm s^{-1}
Plasma-β	β	(24b)	1.8	1.2	–
Wavespeed parameter	ε	(24a)	0.8	1.0	–
Magnetosonic wave speed	u	(75b)	1.2×10^6	2.2×10^7	cm s^{-1}
Cut-off frequency	ω_*	(66)	2.2×10^{-2}	1.4×10^{-3}	s^{-1}
Cut-off period	τ	$2\pi/\omega$	2.9×10^2	4.4×10^3	s
Viscous dissipation[a]	$\dot{E}_\eta$	(84b)	3.0×10^3	3.8×10^{-2}	g cm^{-3} s^{-1}
Resistive dissipation[b]	$\dot{E}_\sigma$	(84c)	4.1×10^2	6.6×10^{-8}	g cm^{-3} s^{-1}
Total dissipation	$\dot{E}$	$\dot{E}_\eta + \dot{E}_\sigma$	3.4×10^3	3.8×10^{-2}	g cm^{-3} s^{-1}
Dissipation per 5-min period[c]	E	$\dot{E}\tau$	1.0×10^6	1.1×10	g cm^{-3}
Energy flux	F	Eu	1.2×10^{12}	2.5×10^7	g cm^{-2} s^{-1}
Ratio to solar radiative flux[d]	F/F_0	–	2.4×10	5.7×10^{-3}	–

[a]Viscous diffusivity: 1.1×10^2 cm^2 s^{-1}.
[b]Resistive diffusivity: 1.0×10^4 cm^2 s^{-1}.
[c]5 min period: $\tau = 3.0 \times 10^2$ s, $\omega = 2.1 \times 10^{-2}$ s^{-1}.
[d]Solar radiative loss: $D = 3.0 \times 10^{33}$ g s^{-1}.
Solar radius: $r = 7.0 \times 10^{10}$ cm.
Solar radiative flux: $F_0 = D/(4\pi r^2) = 4.9 \times 10^{10}$ g cm^{-2} s^{-1}.

Helmholtz number:

$$\Omega = \frac{\omega L}{c} = \frac{\omega RT/g}{\sqrt{\gamma RT}} = \frac{\omega}{g}\sqrt{\frac{RT}{\gamma}}, \tag{67}$$

that varies from $\Omega_1 = (\omega/g)\sqrt{RT_1/\gamma_1} = 0.48$ at the photosphere to $\Omega_2 = (\omega/g)\sqrt{RT_2/\gamma_2} = 7.3$ in the corona. These order of magnitude estimates guide the choice of physical parameters (section 4.2) for the plotting of waveforms of MAG waves (figures 1–3).

4.2. *Reduction of spacing of nodes of the waveforms*

The vertical velocity perturbation of magnetosonic-gravity waves involves three dimensionless parameters. The first is the dimensionless frequency that is given three values (68b) spanning two orders of magnitude:

$$\Omega_* = 0.5 : \qquad \Omega = 0.1, 1, 10, \tag{68a,b}$$

the first below the cut-off (68a) for evanescent waves, the second corresponding roughly to the photosphere and the third to the corona. The range of values (69b) of the wave speed parameter spans one order of magnitude, for comparable sound and Alfvén speeds, or one much larger

than the other:

$$\beta = \frac{p_0}{P_0} = \frac{2}{\gamma\varepsilon}: \qquad \varepsilon \equiv (a/c)^2 = 0.25, 1, 4. \tag{69a,b}$$

The plasma-β or ratio (69a) of gas and magnetic pressures at altitude zero, also involves the adiabatic exponent (70b) for a perfect gas whose molecules have N degrees of freedom (70a):

$$N = 3, 5, 6: \qquad \gamma = 1 + \frac{2}{N} = \frac{5}{3}, \frac{7}{5}, \frac{4}{3}. \tag{70a,b}$$

The values chosen correspond to: (i) fully ionised hydrogen in the corona with three degrees of freedom; (ii) non-ionised hydrogen in the photosphere with diatomic molecules with five degrees of freedom; (iii) for reference multiatomic molecules with atoms not in a row with six degrees of freedom. The altitude is plotted in dimensionless form (47a) over up to 11 scale heights (71a):

$$0 \leq \zeta = \frac{z}{L} \leq 11: \qquad W(\zeta) = \mathrm{Re}\{V_\pm(z;\omega)/V_\pm(0;\omega)\}, \tag{71a,b}$$

and vertical velocity perturbation (63) is normalised to the value at zero altitude (71b) and the real part (63) taken:

$$W(\zeta) = \mathrm{e}^{\zeta/2}\,\mathrm{Re}\left\{\mathrm{e}^{\pm\mathrm{i}\kappa\zeta/2}\,\frac{G(\zeta)}{G(0)}\right\}, \tag{72}$$

in which appears: (i) the confluent hypergeometric function (62) of the first kind

$$\mathrm{G}(\zeta) = \mathrm{F}\left(\frac{1}{2} \mp \frac{\mathrm{i}}{2\kappa} \pm \frac{\mathrm{i}}{2\kappa\gamma} \pm \frac{\mathrm{i}\kappa}{2\gamma};\ 1;\ \mp\mathrm{i}\kappa\left(\beta + \frac{2}{\gamma} + \zeta\right)\right); \tag{73}$$

(ii) the adiabatic exponent γ (70b), the plasma-β (69a) through (69bb) and the dimensionless frequency Ω (68b) through (55b).

The baseline case is taken as the values (74a–c) in (68b), (69b), (70b) that correspond to an Alfvén wave speed $a = 2c$ twice the sound speed at altitude $z = 0$, so that the magnetic field has a strong effect on propagation:

$$\Omega = 10, \quad \varepsilon = 4, \quad \gamma = 5/3: \qquad \kappa = \sqrt{399}, \quad \beta = 0.3, \tag{74a–e}$$

corresponding to (74d,e). Each parameter is varied in turn in figures 1–3.

In figure 1, the plasma-β is fixed (74e) and also the adiabatic exponent (74c) and the dimensionless frequency is given three values (68b). The lowest $\Omega = 0.1 < \Omega_*$ corresponds to an evanescent wave that does not oscillate; the amplitude increases with altitude more slowly than $1/\sqrt{\rho}$ so that the energy ρV^2 decreases and vanishes as $z \to +\infty$. In the case $\Omega = 1$ of propagating waves, there are oscillations with nodes progressively closer as the Alfvén speed reduces with altitude (75a) until the magnetosonic wave speed tends to the sound speed (75b):

$$\lim_{z\to+\infty} A(z) = 0, \qquad \lim_{z\to+\infty} u(z) = \lim_{z\to+\infty} \sqrt{[A(z)]^2 + c^2} = c. \tag{75a,b}$$

For higher frequency $\Omega = 10$, the nodes are closer, leading to larger waveform gradients and stronger dissipation (section 4.3). In figure 2, the dimensionless frequency (74a) and adiabatic exponent (74c) are kept, and the plasma-β at zero altitude is given three values (69a) corresponding to the wave speed parameter (69b) including cases of: (i) Alfvén speed equal to $a = c$ or smaller than $c = 2a$ the sound of speed at altitude $z = 0$; (ii) corresponding larger values of the plasma-β, respectively $\beta = 1.2$ and $\beta = 5$, with the intermediate value representative of solar conditions. For comparable sound and Alfvén speeds, the acoustic oscillations predominate as the altitude increases with constant sound speed and decreasing

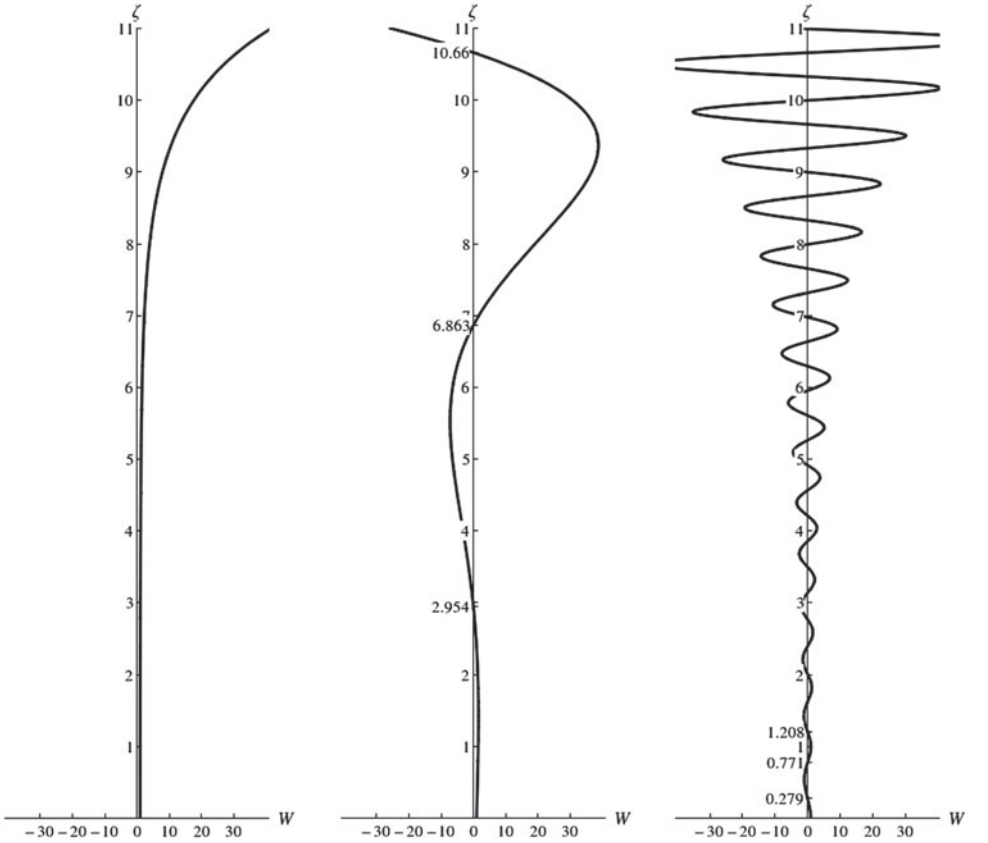

Figure 1. Vertical velocity perturbation W (normalised to the value at zero altitude) plotted against a dimensionless altitude ζ (z normalised to the scale height L) for an altitude range of 11 scale heights. The plots illustrate the effect of dimensionless frequency Ω, for a fixed wave speed parameter ($\varepsilon = 4$) and adiabatic exponent ($\gamma = 5/3$).

Alfvén speed; a large plasma-β leads to a dominant acoustic propagation at lower altitude, whereas a small plasma-β delays it to higher altitudes.

In figure 3, the dimensionless frequency (74a) and wave speed parameter (74b) are kept and the adiabatic exponent is given three values (70b) corresponding to plasma-β value respectively $\beta = 0.3, 0.358, 0.375$. There is little difference between monatomic, diatomic and poliatomic perfect gases; for example, magnetosonic-gravity waves are not much affected by the ionisation of hydrogen across the chromosphere, from diatomic in the photosphere to monatomic in the transition region to the corona.

Figures 1–3 demonstrate the main prediction made in the introduction that the Alfvén speed decreasing with altitude leads to a closer spacing of nodes. The altitudes of the nodes of the waveform, where the velocity perturbation is zero (76a), are denoted by z_n and are ordered in a sequence (76b) of increasing altitude. The decrease in the propagation speed with altitude implies a closer spacing of nodes, for example the ratio of the altitude difference between the third and second and second and first nodes (76c) is less than unity:

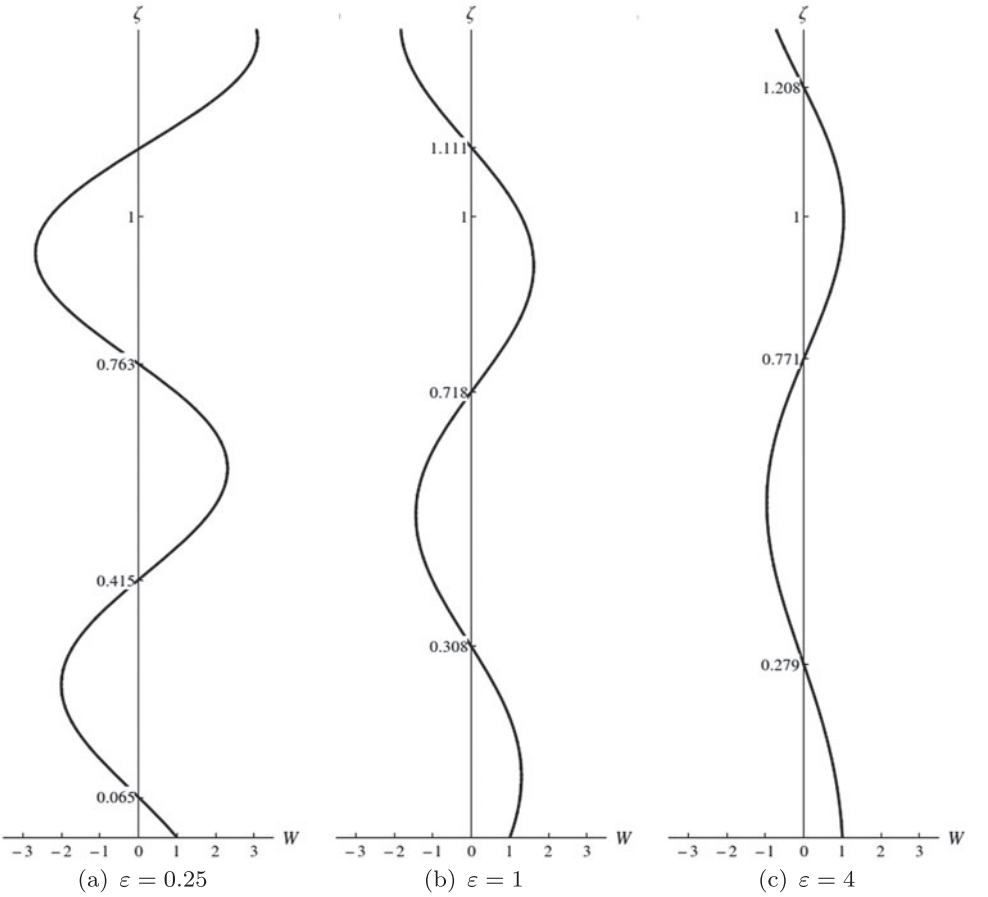

Figure 2. Vertical velocity perturbation W (normalised to the value at zero altitude) plotted against a dimensionless altitude ζ (z normalised to the scale height L) for an altitude range reduced from 11 scale heights in the figure 1 to 1.25 scale heights in the figure 2 to show in detail the first three nodes of the wave form. The plots illustrate the effect of the wave speed parameter at zero altitude, for a fixed dimensionless frequency ($\Omega = 10$) and adiabatic exponent ($\gamma = 5/3$).

$$V(z_n;\omega) = 0\,; \qquad 0 < z_1 < z_2 < \cdots < z_n < \cdots : \qquad \psi = \frac{z_3 - z_2}{z_2 - z_1} < 1\,, \qquad (76a\text{–}c)$$

as can be confirmed from table 2. The assumption of an isothermal atmosphere (15a) implies that the sound speed is constant, whereas the horizontal magnetic field decaying exponentially with altitude (21a) leads to an Alfvén speed (26b) decaying with altitude. If the plasma-β is large (24a); (i) then the wave speed parameter ε in (24a,ba) is small and the Alfvén speed (26b) decays slowly with altitude; (ii) also the sound speed dominates the Alfvén speed in the magnetosonic wave speed (75b). Thus, for large β, the propagation is at nearly constant speed and the ratio (76c) is close to unity at all frequencies, as can be seen from table 2 and figure 2(a). Conversely for small β or large wave speed parameter ε in (24a,ba), the Alfvén speed dominates the sound speed and decays more rapidly with height leading to a closer spacing of nodes as seen in table 2 and in figures 1(c), equivalent to 2(b), equivalent to 3(a) (that are the same with different scales). Ultimately at high altitude, as the Alfvén speed decays to zero (75a) and the magnetosonic wave speed tends to the constant sound speed (75b), the spacing

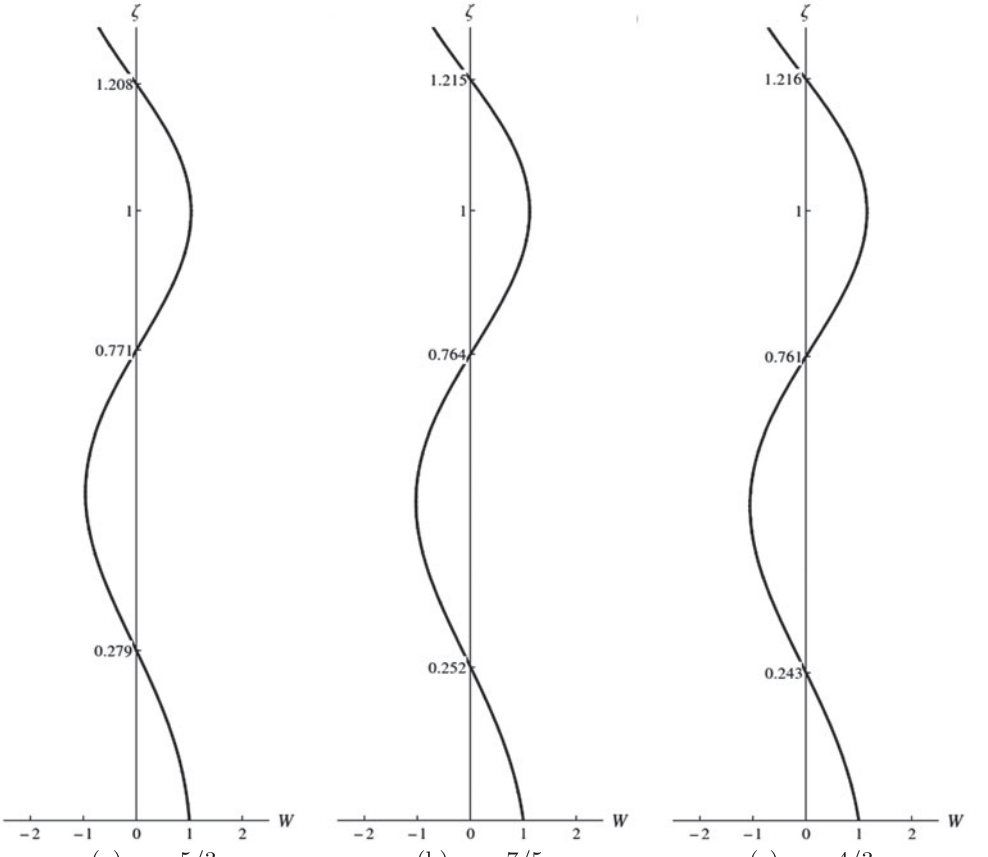

Figure 3. Vertical velocity perturbation W (normalised to the value at zero altitude) plotted against a dimensionless altitude ζ (z normalised to the scale height L) for the same altitude range of 1.25 scale heights as in figure 2, reduced relative to figure 1, to emphasise the first three nodes of the waveform in figure 3. The plots illustrate the effect of adiabatic exponent γ, for a fixed dimensionless frequency ($\Omega = 10$) and plasma-β ($\beta = 4$).

Table 2. Ratio of the spacing of the first three nodes: $\psi = (z_3 - z_2)/(z_2 - z_1)$.

ψ		ε										
		0.25	1	4	9	16	25	36	49	64	81	100
Ω	0.7	0.998	0.996	0.996	0.996	0.996	0.996	0.996	0.996	0.996	0.996	0.996
	1	0.988	0.972	0.972	0.972	0.972	0.972	0.972	0.972	0.972	0.972	0.972
	2	0.984	0.944	0.944	0.944	0.944	0.944	0.944	0.944	0.944	0.944	0.944
	3	0.986	0.929	0.929	0.929	0.929	0.929	0.929	0.929	0.929	0.929	0.929
	5	0.991	0.954	0.910	0.910	0.910	0.910	0.910	0.910	0.910	0.910	0.910
	10	0.994	0.961	0.887	0.887	0.887	0.887	0.887	0.887	0.887	0.887	0.887
	20	0.997	0.971	0.868	0.868	0.868	0.868	0.868	0.868	0.868	0.868	0.868
	30	0.998	0.978	0.917	0.858	0.858	0.858	0.858	0.858	0.858	0.858	0.858
	50	0.999	0.985	0.909	0.848	0.848	0.848	0.848	0.848	0.848	0.848	0.848
	100	0.999	0.991	0.946	0.901	0.838	0.838	0.838	0.838	0.838	0.838	0.838

of nodes becomes constant. Table 2 also shows that the spacing of nodes stabilises for large $\varepsilon \geq 0$ and that the effect of the Helmholtz number is weaker and non-monotonic going through a minimum at $\Omega = 10$ for $\varepsilon = 4$. The waveforms illustrated in figure 1 may be relevant to the observations of low-frequency compressive modes in the corona (Yuan *et al.* 2011). Figure 1 also demonstrates large waveform gradients at high frequencies, leading to strong dissipation that is considered next (section 4.3).

4.3. *Wave dissipation in the transition region and heating of the corona*

The vertical magneto-sonic-gravity wave propagates: (i) a vertical velocity perturbation v_z satisfying (40) whose solution is (63), (64); (ii) an associated horizontal magnetic field perturbation h_x related by (33a) leading to (77b):

$$h_x(z,t) = \int_{-\infty}^{+\infty} H(z,\omega)\mathrm{e}^{-\mathrm{i}\omega t}\mathrm{d}\omega : \qquad \mathrm{i}\omega H = (BV)', \tag{77a,b}$$

where (V, H) denote respectively the spectra of (v_z, h_x) in (42) and (77a). The dissipation of MAG waves is mainly due to the shear viscosity times the square of the rates of strain (78a):

$$\dot{E}_\eta = \eta V'^2, \qquad \dot{E}_\sigma = \frac{1}{\sigma} J^2, \tag{78a,b}$$

and the Joule effect (78b) of the Ohmic resistivity $1/\sigma$ times the electric current; relating (5a) the electric current to the magnetic field (79a) and using the magnetic diffusivity (79b) leads (78b)–(79c) for the Ohmic resistive dissipation:

$$J = \frac{c}{4\pi} H', \qquad \chi = \frac{c^2}{4\pi\mu\sigma} : \qquad \dot{E}_\sigma = \frac{c^2}{16\pi^2\sigma} H'^2 = \frac{\mu\chi}{4\pi} H'^2. \tag{79a–c}$$

Substituting (77a) into (79c) specifies the Ohmic resistive dissipation

$$\dot{E}_\sigma = \frac{\mu\chi}{4\pi} \frac{[(BV)'']^2}{\omega^2} \sim \frac{\mu\chi}{4\pi} \left(\frac{BV''}{\omega}\right)^2 \tag{80}$$

in terms of the velocity, that may be compared with the shear viscous dissipation (78a).

Using the differentiation formula (Abramowitz and Stegun 1964) for the confluent hypergeometric function (62):

$$\frac{\mathrm{d}}{\mathrm{d}\eta} \mathrm{F}(b;1;\eta) = b\eta\, \mathrm{F}(b+1;2;\eta), \tag{81}$$

specifies the rate-of-strain associated with the vertical velocity perturbation spectrum:

$$V'_\pm(z;\omega) = \mathrm{e}^{z/2L} e^{\pm \mathrm{i}kz} \left[\left(\frac{1}{2L} \pm \mathrm{i}\kappa \right) \mathrm{F}(b;1;\eta) + b \frac{\mathrm{d}\eta}{\mathrm{d}z} \mathrm{F}(b+1;2;\eta) \right], \tag{82}$$

where b is a constant (61b) and η depends on altitude (59a), (50a), (47a):

$$\eta = \mp \mathrm{i}\kappa \left(\beta + \frac{2}{\gamma} + \frac{z}{L} \right), \qquad \frac{\mathrm{d}\eta}{\mathrm{d}z} = \mp \frac{\mathrm{i}\kappa}{L} = \mp \mathrm{i}2k, \tag{83}$$

and the effective vertical wavenumber (57a) was used. The product of (61b) and (83) that appears in the rate-of-strain (82) leads for $\kappa \gg 1$ to the scaling (84a):

$$V' \sim \frac{\kappa^2 V}{2\gamma L} : \qquad \dot{E}_\eta \sim \eta \left(\frac{\kappa^2 V}{2\gamma L} \right)^2, \qquad \dot{E}_\sigma \sim \frac{\mu\chi}{4\pi} \left(\frac{\kappa^4 BV}{4\omega\gamma^2 L^2} \right)^2, \tag{84a–c}$$

that is applied to the viscous (78a) and resistive (80) dissipation leading respectively to (84b) and (84c). For gradual dissipation on the scale of a wave period, it is permissible to use the non-dissipative waveform (63) to calculate the rates of viscous (84b) and resistive (84c) dissipation.

The previous value of the dimensionless frequency $\Omega = 7.2$ for magnetosonic-gravity waves corresponds (55b) to the dimensionless vertical effective wavenumber $\kappa = 1.4 \times 10$. Using $\eta = 1.1 \times 10^2$ cm^2 s^{-1} for the shear viscosity (Campos 1984) and $V \sim 1.0 \times 10^6$ cm s^{-1} for the typical velocities in the transition region, the rate of viscous dissipation (84b) varies between $\dot{E}_{\eta 1} \sim \eta(\kappa^2 V/2L_1)^2 = 3.0 \times 10^3$ g cm^{-3} s^{-1} in the photosphere and $\dot{E}_{\eta 2} \sim \dot{E}_{\eta 1}(L_1/L_2)^2 = 3.8 \times 10^{-2}$ g cm^{-3} s^{-1} in the corona. Using $\chi = 1.0 \times 10^4$ cm^2 s^{-1} for the resistive diffusivity (Cowling 1980), the rate of resistive dissipation (84c) varies from $\dot{E}_{\sigma 1} \sim (\mu\chi/4\pi)(\kappa^4 B_1 V/4\omega\gamma^2 L_1^2)^2 = 4.1 \times 10^2$ g cm^{-3} s^{-1} in the photosphere to $\dot{E}_{\sigma 2} \sim \dot{E}_{\sigma 1}(L_1/L_2)^4 = 6.6 \times 10^{-8}$ g cm^{-3} s^{-1} in the corona. Thus the energy dissipation is dominated by viscosity in the corona $\dot{E}_2 \sim \dot{E}_{\eta 2} = 3.8 \times 10^{-2}$ g cm^{-3} s^{-1} where the magnetic field is weak $B_2 = 20$ G and resistive diffusivity makes a contribution in the photosphere $\dot{E}_1 = \dot{E}_{\eta 1} + \dot{E}_{\sigma 1} = 3.4 \times 10^3$ g cm^{-3} s^{-1}. The use of constant viscous and resistive diffusivity implies that these dissipation rates are orders of magnitude. The dissipated energy in a 5 min period $\tau = 3.0 \times 10^2$ s is $E_1 = \tau \dot{E}_1 = 1.0 \times 10^6$ g cm^{-3} in the photosphere and $E_2 = \tau \dot{E}_2 = 1.1 \times 10$ g cm^{-3} in the corona. The magnetosonic wave speed $u = \sqrt{a^2 + c^2}$ varies from $u_1 = \sqrt{a_1^2 + c_1^2} = 1.2 \times 10^6$ cm s^{-1} at the photosphere to $u_2 = \sqrt{a_2^2 + c_2^2} = 2.2 \times 10^7$ cm s^{-1} in the corona. The corresponding energy flux is $F_1 = E_1 u_1 = 1.2 \times 10^{12}$ g cm^{-2} s^{-1} in the photosphere or low transition region and $F_2 = E_2 u_2 = 2.5 \times 10^7$ g cm^{-2} s^{-1} in the high transition region and corona. The total solar radiative loss $D = 3.0 \times 10^{33}$ g s^{-1}, divided over the solar disk with radius $r = 7.0 \times 10^{10}$ cm, leads to the energy flux $F = D/(4\pi r^2) = 4.9 \times 10^{10}$ g cm^{-2} s^{-1}. It follows that: (i) local dissipative heating in the corona is insufficient to compensate for solar radiative losses $F_2/F = 5.2 \times 10^{-4}$; (ii) the dissipation in the low transition region is more than sufficient to compensate for solar radiative losses $F_1/F = 2.4 \times 10$. Thus the dissipation of magnetosonic-gravity waves can heat the transition region. The higher temperatures in the corona cannot be explained by thermal conduction from the transition region since heat cannot pass from a colder to a hotter body with supply mechanical work.

5. Discussion

When considering magneto-atmospheric waves, it is convenient to distinguish four types of theories, depending on the combination of two criteria, namely whether: (a) stratification due to gravity is or is not taken into account; (b) the external magnetic field is assumed to be uniform or not. The four types of theories I–IV are briefly discussed in the sequence: (I) MHD waves in an homogeneous medium under a uniform magnetic field; (II) flux tube modes in a discontinuous magnetic field; (III)–(IV) MAG waves in an atmosphere stratified by gravity in the presence of an uniform (III) or non-uniform (IV) external magnetic field. The simplest theory (I) assumes a uniform magnetic field and an homogeneous medium (in the sense that the mass density and sound speed are constant), leading to MHD waves. This neglects both the magnetic structures observed in the solar atmosphere and the variation of physical properties with altitude. It does serve to identify three modes (Alfvén and Falthammar 1962, Campos 1977): decoupled transverse Alfvén waves and coupled compressive slow and fast modes in

adiabatic conditions; a fourth entropy mode exists in the presence of heat exchanges. It shows that the slow and fast modes become a second-order magnetosonic wave if the magnetic field is orthogonal to the direction of propagation. It also shows that if the magnetic pressure is much larger than the gas pressure, the slow modes are acoustic waves guided along magnetic field lines.

The last result points to the next theory (II), namely modes in magnetic flux tubes (Spruit 1981, 1982). This kind of theory is supported by the observation of magnetic structures in the solar atmosphere, such as flux tubes in intergranular lanes in the photosphere, spicules in the corona and loops crossing from the chromosphere through the transition region to the corona, where they are most visible as bright structures. Current theories of flux tube modes assume a magnetic field with different magnitudes inside and outside; taking into account field-aligned non-uniformity allows the consideration of the ratios of the periods of the wavemodes P_2/P_1 on coronal loops opening the promising subject of magnetohelioseismology (Andries *et al.* 2009). The non-integral ratios of the first four periods of Alfvén-gravity waves (Campos 1989a) had earlier been found to agree with the observations of sunspot umbral oscillations (Bhatnagar *et al.* 1972, Balthasar and Wiehr 1984).

In the theories of type I and type II without stratification: (a) the sound and Alfvén speeds are constant, and hence all other wave speeds, e.g. the magnetosonic or the tube speed, are constant; (b) since all wave speeds are constant, the waves are sinusoidal functions of altitude, there is equipartition of energies (e.g. kinetic and magnetic), the energy flux equals the energy density times the wave speed. The properties (b) generally do not hold if the wave speed is non-uniform. In the solar atmosphere, the sound speed varies (table 1) from about 9 km/s in the chromosphere to 160 km/s in the low corona. The Alfvén speed varies from about 8 km/s in intergranular lanes to 160 km/s in the transition region, and is higher in the corona as the density decreases. This calls into question the consideration of constant wave speeds. A third type of theory (III) assumes a uniform magnetic field in an isothermal atmosphere under uniform gravity, so that the sound speed is constant and the Alfvén speed increases with altitude on twice the scale height $A(z) \sim ae^{z/2L}$. This horizontally homogeneous model averages out all magnetic structures but does retain a significant altitude dependence, leading to MAG waves (Scheuer and Thomas 1981, Campos 1987).

The MAG waves are sinusoidal and are completely described by a dispersion relation (Stein and Leibacher 1974) in the WKB-approximation that the wavelength is small compared with the lengthscale of variation of properties of the medium, that is the scale height for an atmosphere. For a wave period of 5 min, or 300 s, the sound or Alfvén speed of 8 km/s in the chromosphere would correspond to a "wavelength" $\lambda = 2400$ km, about ten times the scale height $L = 200$ km. It is clear that the WKB approximation and the assumption of sinusoidal waves with a constant wave speed fail by about an order of magnitude in the solar photosphere and chromosphere; a "wavelength" less than the scale height $L = 200$ km would correspond to periods of less than $\tau \leq 30$ s, that are a small part of the energy spectrum of solar radiation. In conclusion, the theories of type I and II without stratification are of limited use in the low solar atmosphere since for periods of 1 min or more the local vertical wavelength is larger than the atmospheric scale height and the waveforms are far from sinusoidal in altitude.

In the low corona, the sound or Alfvén speed of 160 km/s for a wave with a 5 min or 300 s period would correspond to a "wavelength" of 48, 000 km comparable to the scale height $L = 55, 000$ km, and therefore at the limits of WKB theory. This suggests that the consideration of variable wave speed, and non-sinusoidal waveforms, is essential in the solar atmosphere, in particular for magnetic modes affected by the strong variations of the Alfvén speed with altitude. The theories of type I and II apply best in the corona since the large scale

height $L \sim 55,000$ km allows for sinusoidal waves over wavelengths $\lambda^2 > L^2$ of up to $\lambda \leq 15,000$ km. Thus the theories of flux tube modes without stratification may model the coronal part of magnetic flux tubes but will be more limited if extended to the foot points in the chromosphere. Similarly sinusoidal waves with constant wave speeds are not an adequate model for wave propagation across the whole solar atmosphere from the photosphere to the corona. It is not surprising that these theories predict that neither acoustic nor Alfvén waves can heat the chromosphere, due to the effects of cut-off frequencies and strong reflections (Osterbrock 1961).

The hydrodynamic turbulence and ionised inhomogeneities in the solar chromosphere can act as wave sources (Kulsrud 1955, Campos 2008), both for the sun and stars (Campos 2011b, Campos 2011c). As mentioned in the introduction, the acoustic modes can be associated with spicules and the mass balance including mass supply to the solar wind and return downflows through the transition region (Beckers 1972, Campos 1984, De Pontieu *et al.* 2004). The magnetic modes should be responsible for the solar energy balance since regions of strong magnetic field are observed to be hotter and brighter; the alternative to heating of the atmosphere by wave dissipation is magnetic reconnection (Parker 1979, Priest 1982) and other mechanisms involving change of the topology of the magnetic field and release of magnetic energy. The heating of the solar chromosphere by viscous and resistive dissipation of Alfvén-gravity waves becomes feasible (Campos and Mendes 1995) if it is taken into account that (i) due to the fast increase of the Alfvén speed with altitude, the waves are not sinusoidal or periodic vertically, and the waveforms are stretched leading to significant waveform gradients; (ii) the associated velocity and magnetic field gradients, that is rates-of-strains and electric currents, in the presence of viscous and resistive dissipation lead to atmospheric heating sufficient to compensate for chromospheric radiative losses. These conclusions would not be possible assuming sinusoidal Alfvén waves.

The same arguments suggest that the dissipation of Alfvén waves is a less effective mechanism to heat the transition region to the corona (Campos and Mendes 1999), because the waveform gradients are too small as the waveform becomes too stretched by the large Alfvén speed. An Alfvén speed of 8 km/s implies that the distance $D = 2,000$ km from the photosphere to the transition region is covered in about 250 s; the same distance in the corona is covered in 13 s at an Alfvén speed of 160 km/s. There must be a significant energy flux of Alfvén waves across the solar corona, at least a part of which goes to the solar wind where waves are observed with large amplitudes (Belcher and Davis 1971, Campos *et al.* 1999). However, the reported observations of a large energy flux of Alfvén waves in the solar corona (Tomczyk *et al.* 2007) have been contested on two grounds that: (i) the observed transversal motions are due to kink rather than torsional modes (Van Doorsselaere, Nakariakov *et al.* 2008); (ii) the energy flux is overestimated (Goossens *et al.* 2013). Coronal heating theories not based on wave dissipation include nano-flares (Parker 1979) and magnetic reconnection (Priest 1982).

A different mechanism may be needed to heat the solar corona, bearing in mind that closed regions like loops are bright and hot, and open regions like coronal holes are dark and cool. A distinction is that closed regions have an horizontal magnetic field where occurs critical layer conversion between hydrodynamic and hydromagnetic modes (Adam 1977, Campos 1988), and intense dissipation. The magnetic field is nowhere horizontal in a coronal hole and critical layer absorption of magnetosonic waves does not occur ; instead fourth-order hydromagnetic waves (Scheuer and Thomas 1981, Campos and Saldanha 1991) propagate out of coronal holes and transfer energy to the solar wind causing high-speed particle streams.

Table 3. Role of MAG waves in the solar mass and energy balances.

Region/Wave	Acoustic-gravity	Alfvén-gravity	Magnetosonic-gravity	Hydromagnetic-gravity
Flares/CMEs	MHD shock waves			
Solar Wind	mass flux	Convection with the wind	Thermal expansion	High-speed streams
Corona	Spicules guided by the magnetic field	fast propagation	Heating of loops	Acceleration of particles
Transition region	Decoupled	propagation	Dissipation at critical layer	Mode conversion
Chromosphere	Growth to nonlinear amplitude	Dissipative heating	Filtering	Coupled propagation
Photosphere	Wave generation by hydromagnetic turbulence and ionised inhomogeneities			

These considerations suggest a simple assignment of roles for each MHD wave mode in the solar mass and energy balances (table 3): (i) hydromagnetic turbulence and ionised inhomogeneities generate all modes in the photosphere; (ii) acoustic modes leak to the corona and appear as spicules leading to the mass balance and average solar wind; (iii) Alfvén-gravity waves can heat the chromosphere if the non-sinusoidal waveform shearing due to the fast increase in Alfvén speed with altitude is taken into account; (iv) the closed magnetic regions, like loops in the corona, are bright and hot due to critical layer absorption of magnetosonic-gravity waves in nearly horizontal magnetic fields; (v) critical layers do not occur in open magnetic regions like coronal holes, that are dark and cold since hydromagnetic-gravity waves are not absorbed and propagate outward to accelerate high-speed particle streams in the solar wind; (vi) the MAG waves in the solar wind have an additional effect of convection, in the sense that they propagate in a moving medium with background velocity that is non-negligible, and may be comparable to or larger than the wave speed; (vii) the coronal mass ejections and large energy eruptions associated with solar flares would generate MHD waves with large amplitude or MHD shock waves. The preceding simple global picture of the role of waves in the solar atmosphere: (i) can be challenged by any specific theory of local phenomena, making a consensus difficult or unlikely; (ii) does attempt to bring some order to multiplicity of explanations of partial phenomena.

For example, the heating of coronal loops by waves can be explained in two alternative way in the context of: (i) magnetic flux tubes by modes propagating longitudinally and reflected from the footpoints several times, thus repeatedly heating the plasma until substantially dissipated; (ii) magneto-atmospheric waves because the mode conversion at the critical layer and associated intense energy exchange with the atmosphere occur only for a horizontal magnetic field, that exists near the top of a magnetic loop and not in a coronal hole. Both theories (i) and (ii) can explain the difference between bright, hot, coronal loops and dark, cold, coronal holes. Also the two physical mechanisms are compatible and complementary since (ii) critical layer absorbtion near the top of a magnetic loop can enhance the (i) dissipation of wave modes with multiple reflections between the footpoints. The MAG waves in the solar wind are affected by convection with the mean flow since the background velocity of the solar wind can be comparable to or larger than the wave speed. Critical layers involving the absorption, amplification, reflection or mode conversion can occur for linear and nonlinear waves (Bretherton 1966, Lighthill 1978), hydrodynamic and hydromagnetic waves (Adam 1977, Campos 1985, Campos 1988), viscous and resistive dissipation (Yanowitch 1977, Campos 1989b, Campos 1993) and moving media (Campos and Gil 1999, Campos and Isaeva 1999).

All the MHD wave modes can lead to oscillations in reflecting conditions, and the large gradients in mass density and magnetic field act as gradual reflectors; this relates to the fourth type of wave theories (IV) including effects of stratification and non-uniform magnetic fields. Wave-like oscillations are observed in most magnetic structures in the solar atmosphere, for example in sunspot umbras and coronal loops. The natural frequencies of harmonics are not multiples of the fundamental frequency, proving that the waves are not sinusoidal and the wave speeds are not constant. In the case of sunspot umbral oscillations, the periods of harmonics are larger than multiples of the fundamental (Bhatnagar *et al.* 1972, Schroeter and Soltau 1976, Balthasar and Wiehr 1984); this implies that the wave speed increases with altitude, and the profile corresponding to Alfvén-gravity waves in an isothermal atmosphere under a uniform magnetic field leads to the correct wave periods (Campos 1989a). The harmonics of oscillations in coronal loops have lower periods than the multiples of the fundamental mode (Van Doorsselaere *et al.* 2007, Srivastava *et al.* 2008); this shows that the wave speed decreases with altitude, as is the case for the Alfvén speed (26b) in an isothermal atmosphere (15a) under an horizontal magnetic field decaying exponentially with altitude on twice the scale height (21a). If the wave speed is constant, the frequencies of the harmonics or overtones are multiples of the fundamental. If the wave speed increases with altitude, the frequencies of the harmonics are less than multiples and they are larger than multiples if the wave speed decreases with altitude.

The contrast between oscillations in sunspot umbras and coronal loops, that have harmonics respectively higher and lower than the fundamental, shows how sensitive wave properties are to non-uniform wave speed profiles. The sound speed depends on temperature and composition, and the Alfvén speed on mass density and magnetic field. The MAG wave equation is a partial differential equation whose coefficients depend on the sound and Alfvén speeds and on the scale heights of variation of the mass density and magnetic field. Analytical solutions can be obtained only for relatively simple forms of the variable coefficients of the wave equation; since sinusoidal solutions do not exist, special functions are needed. There are sophisticated two (Gabriel 1976) and three (Stix 1989) dimensional models of the magnetic field in the solar atmosphere, leading to numerical solutions for waves. The analytical solutions could be used as simpler, particular benchmark cases for numerical codes. The critical element in helioseismology is the dependence of the sound speed with depth, that is related to the internal structure of the sun (Gough 1985). The quality and quantity of observational data on the solar atmosphere opens the prospect of heliomagnetoseismology. The critical factor in its implementation is the dependence on the sound and Alfvén speeds on altitude (or other relevant coordinate in the direction of inhomogeneity) because the wave speeds: (i) determine the wave properties, like waveforms for propagating waves and periods for standing modes; (ii) are related to the atmospheric properties and magnetic fields. In this context, the best wave diagnostic is the variation with altitude of wave speeds, amplitudes and phases. The variation with altitude of horizontal velocities in the chromosphere (Beckers and Canfield 1975) allowed the identification of Alfvén-gravity waves (Campos 1998). Modern satellite observations can provide more altitude dependences as wave mode diagnostic and magnetohelioseismology tool (Andries *et al.* 2009).

Acknowledgements

This work was supported by FCT (Foundation for Science and Technology), through IDMEC (Institute of Mechanical Engineering), under LAETA, project UID/EMS/50022/2013. The authors acknowledge the benefit of comments from the two reviewers.

Disclosure statement

No potential conflict of interest was reported by the authors.

ORCID

L. M. B. C. Campos http://orcid.org/0000-0003-2431-3274
A. C. Marta http://orcid.org/0000-0002-9399-7967

References

Abramowitz, M., and Stegun, I.A. (Eds.), *Handbook of Mathematical Functions with Formulas, Graphs, and Mathematical Tables*, 1964 (National Bureau of Standards: Washington).
Adam, J.A., On the occurrence of critical levels in solar magnetohydrodynamics. *Solar Phys.* 1977, **52**, 293–307.
Alfvén, H., Granulation, magnetohydrodynamic waves and the heating of the solar corona. *Mon. Not. Roy. Astron. Soc.* 1947, **107**, 211–219.
Alfvén, H., *Cosmical Electrodynamics*. International series of monographs on physics, 1950 (Clarendon Press: Oxford).
Alfvén, H. and Falthammar, C.G., *Cosmical Electrodynamics*, 1962 (Oxford University Press: London).
Andries, J., Van Doorsselaere, T., Roberts, B., Verth, G., Verwichte, E. and Erdélyi, R., Coronal seismology by means of kink oscillation overtones. *Space Sci. Rev.* 2009, **149**, 3–29.
Aschwanden, M.J., Fletcher, L., Schrijver, C.J. and Alexander, D., Coronal loop oscillations observed with the transition region and Coronal Explorer. *Astrophys. J.* 1999, **520**, 880–894.
Athay, R.G., *The Solar Chromosphere and Corona: Quiet Sun*, Vol. 53, Astrophysics and space science library,1976 (D. Reidel Publishing Company: Dordrecht). ISBN:9789027702449.
Athay, R.G. and Holzer, T.E., The role of spicules in heating the solar atmosphere. *Astrophys. J.* 1982, **255**, 743–752.
Balthasar, H. and Wiehr, E., Umbral oscillations measured in the Stokes-V inversion point. *Solar Phys.* 1984, **94**, 99–103.
Banerjee, D., Erdélyi, R., Oliver, R. and O'Shea, E., Present and future observing trends in atmospheric magnetoseismology. *Solar Phys.* 2007, **246**, 3–29.
Beckers, J.M., Solar spicules. *Solar Phys.* 1968, **3**, 367–433.
Beckers, J.M., Solar spicules. *Annu. Rev. Astron. Astrophys.* 1972, **10**, 73–100.
BeckersJ.M. and CanfieldR.C., *Horizontal velocities in the solar chromosphere*, Technical report AFCRL-75-486, Air Force Cambridge Research Laboratory, 1975.
Belcher, J.W. and Davis, L., Large-amplitude Alfvén waves in the interplanetary medium, 2. *J. Geophys. Res.* 1971, **76**, 3534–3563.
Bhatnagar, A., Livingston, W.C. and Harvey, J.W., Observations of sunspot umbral velocity oscillations. *Solar Phys.* 1972, **27**, 80–88.
Biermann, L., ber die Ursache der chromosphrischen Turbulenz und des UV-Exzesses der Sonnenstrahlung [The cause of chromospheric turbulence and UV excess of solar radiation]. *Z. Astrophys.* 1948, **25**, 161–177.
Bray, R.J. and Loughhead, R.E., *The Solar Chromosphere*, 1974 (Chapman & Hall: London). ISBN:9780412107306.
Bretherton, F.P., Baroclinic instability and the short wavelength cut-off in terms of potential vorticity. *Q. J. Roy. Meteor. Soc.* 1966, **92**, 335–345.
Bruzek, A., Durrant, C.J. (Eds.), *Illustrated Glossary for Solar and Solar-terrestial Physics*. Vol. 69, Astrophysics and space science library, 1977 (D. Reidel Publishing Company: Dordrecht). ASIN:B0016O3PTC.
Burlaga, L.F. and Turner, J.M., Microscale Alfvén waves in the solar wind at 1 AU. *J. Geophys. Res.* 1976, **81**, 73–77.
Campos, L.M.B.C., On the generation and radiation of magneto-acoustic waves. *J. Fluid Mech.* 1977, **81**, 529–549.
Campos, L.M.B.C., On waves in non-isothermal, compressible, ionized and viscous atmospheres. *Solar Phys.* 1983, **82**, 355–368.
Campos, L.M.B.C., On a theory of solar spicules and the atmospheric mass balance. *Mon. Not. Roy. Astron. Soc.* 1984, **207**, 547–574.
Campos, L.M.B.C., On vertical hydromagnetic waves in a compressible atmosphere under an oblique magnetic field. *Geophys. Astrophys. Fluid Dyn.* 1985, **32**, 217–272.
Campos, L.M.B.C., On waves in gases. Part II: Interaction of sound with magnetic and internal modes. *Rev. Mod. Phys.* 1987, **59**, 363–463.
Campos, L.M.B.C., On the properties of hydromagnetic waves in the vicinity of critical levels and transition layers. *Geophys. Astrophys. Fluid Dyn.* 1988, **40**, 93–132.
Campos, L.M.B.C., On oscillations in sunspot umbras and wave radiation in stars. *Month. Not. Roy. Astron. Soc.* 1989a, **241**, 215–229.

Campos, L.M.B.C., On the dissipation of atmospheric Alfvén waves in uniform and non-uniform magnetic fields. *Geophys. Astrophys. Fluid Dyn.* 1989b, **48**, 193–215.
Campos, L.M.B.C., Comparison of exact solutions and the phase mixing approximation for dissipative Alfvén waves. *Eur. J. Mech. B-Fluid* 1993, **12**, 187–216.
Campos, L.M.B.C., On hydromagnetic waves in atmospheres with application to the sun. *Theor. Comp. Fluid Dyn.* 1998, **10**, 37–70.
Campos, L.M.B.C., On the generation, propagation and radiation of magneto-acoustic-gravity waves. *Geophys. Astro. Fluid* 2008, **102**, 51–74.
Campos, L.M.B.C., On magnetoacoustic-gravity-inertial (MAGI) waves I. Generation, propagation, dissipation and radiation. *Mon. Not. Roy. Astron. Soc.* 2011a, **410**, 717–734.
Campos, L.M.B.C., On magnetoacoustic-gravity-inertial (MAGI) waves II. Application to magnetic and rotating stars. *Mon. Not. Roy. Astron. Soc.* 2011b, **410**, 735–761.
Campos, L.M.B.C., On magnetoacoustic-gravity-inertial (MAGI) waves II. Application to magnetic and rotating stars. *Mon. Not. Roy. Astron. Soc.* 2011c, **410**, 735–761.
Campos, L.M.B.C. (Ed.), *Transcendental Representations with Applications to Solids and Fluids*. Vol. 2, Mathematics and physics for science and technology, 2012 (CRC Press: New York). ISBN:9781439834312.
Campos, L.M.B.C., *Generalized Calculus with Applications to Matter and Forces*. Vol. 3, Mathematics and physics for science and technology, 2014 (CRC Press: New York). ISBN:9781420071153.
Campos, L.M.B.C. and Gil, P.J.S., On Alfvén waves in a flowing atmosphere. *Phys. Plasmas* 1999, **6**, 3345–3357.
Campos, L.M.B.C. and Isaeva, N.L., On Alfvén waves in a radial flow and magnetic field. *J. Plasma Phys.* 1999, **62**, 1–33.
Campos, L.M.B.C. and Isaeva, N.L., On the critical layer of Alfvén waves in the solar wind. *J. Plasma Phys.* 2004, **70**, 271–302.
Campos, L.M.B.C., Isaeva, N.L. and Gil, P.J.S., On the reflection of Alfvén waves in the inhomogeneous solar wind. In *Nonlinear MHD Waves and Turbulence*. Vol. 536, Lecture notes in physics, edited by T. Passot, P.L. Sulem, pp. 104–159, 1999 (Springer: Berlin Heidelberg).
Campos, L.M.B.C. and Mendes, P.M.V.M., On the compatibility of Alfvén wave heating of the chromosphere, transition region and corona. *Mon. Not. Roy. Astron. Soc.* 1995, **276**, 1041–1051.
Campos, L.M.B.C. and Mendes, P.M.V.M., On dissipative Alfvén waves in atmospheres with steep temperature gradients. *Geophys. Astrophys. Fluid Dyn.* 1999, **91**, 103–130.
Campos, L.M.B.C. and Saldanha, R., On oblique magnetohydrodynamic waves in an atmosphere under a magnetic field of arbitrary direction. *Geophys. Astrophys. Fluid Dyn.* 1991, **56**, 237–266.
Carathéodory, C., *Theory of Functions of a Complex Variable*. Vol. 1–2, 1950 (Verlag Birkhauser: Basel). ISBN:9780821828311.
Copson, E.T., *Theory of Functions of a Complex Variable*, 1935 (Oxford University Press: London). ISBN:9780198531456.
Cowling, T.G., *Magnetohydrodynamics*. 2nd ed., Monographs on astronomical subjects, 1980 (Hilger: Bristol). ISBN: 9780852743003.
De Moortel, I., Ireland, J., Hood, A.W. and Walsh, R.W., The detection of 3 & 5 min period oscillations in coronal loops. *Astron. Astrophys.* 2002, **387**, L13–L16.
De Moortel, I. and Nakariakov, V.M., Magnetohydrodynamic waves and coronal seismology: an overview of recent results. *Phil. Trans. R. Soc. A* 2012, **370**, 3193–3216.
De Pontieu, B., McIntosh, S.W., Carlsson, M., Hansteen, V.H., Tarbell, T.D., Schrijver, C.J., Title, A.M., Shine, R.A., Tsuneta, S., Katsukawa, Y., Ichimoto, K., Suematsu, Y., Shimizu, T. and Nagata, S., Chromospheric Alfvénic waves strong enough to power the solar wind. *Science* 2007, **318**, 1574–1577.
De Pontieu, B., Erdélyi, R. and James, S.P., Solar chromospheric spicules from the leakage of photospheric oscillations and flows. *Nature* 2004, **430**, 536–539.
De Pontieu, B. and McIntosh, S.W., Quasi-periodic propagating signals in the solar corona: The signature of magnetoacoustic waves or high-velocity upflows? *Astrophys. J.* 2010, **722**, 1013–1029.
DeForest, C.E. and Gurman, J.B., Observation of quasi-periodic compressive waves in solar polar plumes. *Astrophys. J.* 1998, **501**, L217–L220.
Engvold, O., Tandberg-Hanssen, E. and Reichmann, E., Evidence for systematic flows in the transition region around prominences. *Solar Phys.* 1985, **96**, 35–51.
Erdélyi, A. (Ed.), *Higher Transcendental Functions*. Vol. 3, 1953 (McGraw-Hill: New York). B000J2W8DQ.
Ferraro, C.A. and Plumpton, C., Hydromagnetic waves in a horizontally stratified atmosphere. *Astrophys. J.* 1958, **127**, 459–476.
Fujimura, D. and Tsuneta, S., Properties of magnetohydrodynamic waves in the solar photosphere obtained with Hinode. *Astrophys. J.* 2009, **702**, 1443–1457.
Gabriel, A.H., A magnetic model of the solar transition region. *Phil. Trans. R. Soc. Lond. A* 1976, **281**, 339–352.
Goossens, M., Van Doorsselaere, T., Soler, R. and Verth, G., Energy content and propagation in transverse solar atmospheric waves. *Astrophys. J.* 2013, **768**, 191–779.
Gough, D.O. (Ed.), *Seismology of the Sun and the Distant Stars*. Vol. 169, NATO ASI series. Series C: mathematical and physical sciences, 1985 (D. Reidel Publishing Company: Dordrecht).

Herlofson, N., Magneto-hydrodynamic waves in a compressible fluid conductor. *Nature* 1950, **165**, 1020–1021.
Ince, E.L., *Ordinary Differential Equations*, 1956 (Dover: Mineola). ISBN:9780486603490.
Jess, D.B., Mathioudakis, M., Erdélyi, R., Crockett, P.J., Keenan, F.P. and Christian, D.J., Alfvén waves in the lower solar atmosphere. *Science* 2009, **323**, 1582–1585.
Kamke, E., *Differentialgleichungen. Loesungsmethoden Und Loesungen II. Partielle Differentialgleichungen Erster Ordnung Fuer Eine Gesuchte Funktion* [Differential Equations: Volume II Solution methods and solutions], 1944 (Chelsea: Leipzig). ISBN:9780828402774.
Klein, F., Über Körper, welche von confocalen Flächen zweiten Grades begränzt sind [About bodies which are bounded by second degree confocals]. *Math. Ann.* 1881, **18**, 410–427.
Kulsrud, R.M., Effect of magnetic fields on generation of noise by turbulence. *Astrophys. J.* 1955, **121**, 461–480.
Kuridze, D., Morton, R.J., Erdélyi, R., Dorrian, G.D., Mathioudakis, M., Jess, D.B. and Keenan, F.P., Transverse oscillations in chromospheric mottles. *Astrophys. J.* 2012, **750**, 51–55.
Leroy, B., Propagation of waves in an atmosphere in the presence of a magnetic field. II – The reflection of Alfvén waves. *Astron. Astrophys.* 1980, **91**, 136–146.
Lighthill, M.J., *Notes on the hypergeometric function*. Lecture notes – private communication, 1977 (Imperial College: London).
Lighthill, M.J., *Waves in Fluids*, 1978 (Cambridge University Press: Cambridge). ISBN:9780521216890.
McIntosh, S.W., De Pontieu, B., Carlsson, M., Hansteen, V., Boerner, P. and Goossens, M., Alfvénic waves with sufficient energy to power the quiet solar corona and fast solar wind. *Nature* 2011, **475**, 477–480.
McLellan, A. and Winterberg, F., Magneto-gravity waves and the heating of the solar corona. *Solar Phys.* 1968, **4**, 401–408.
Nye, A.H. and Thomas, J.H., Solar magneto-atmospheric waves. I – an exact solution for a horizontal magnetic field. *Astrophys. J.* 1976, **204**, 573–588.
Ofman, L., Romoli, M., Poletto, G., Noci, G. and Kohl, J.L., Ultraviolet coronagraph spectrometer observations of density fluctuations in the solar wind. *Astrophys. J.* 1997, **491**, L111–L114.
Osterbrock, D.E., The heating of the solar chromosphere, plages, and corona by magnetohydrodynamic waves. *Astrophys. J.* 1961, **134**, 347–388.
Parker, E.N., *Cosmical Magnetic Fields: Their Origin and their Activity*, 1979 (Oxford University Press: London), 858 p.
Pedlosky, J., *Geophysical Fluid Dynamics*. 2nd ed., 1990 (Springer-Verlag: New York). ISBN: 9780387963877.
Pneumann, G. and Kopp, R., Downflow of spicular material and transition region models. *Astron. Astrophys.* 1977, **55**, 305–306.
Priest, E.R., *Solar Magnetohydrodynamics*, 1982 (Springer: New York). ISBN:9789027713742.
Roberts, B., Waves and oscillations in the corona. *Solar Phys.* 2000, **193**, 139–154.
Scheuer, M.A. and Thomas, J.H., Umbral oscillations as resonant modes of magneto-atmospheric waves. *Solar Phys.* 1981, **71**, 21–38.
Schroeter, E.H. and Soltau, D., On the time behaviour of oscillations in sunspot umbrae. *Astron. Astrophys.* 1976, **49**, 463–465.
Schwarzschild, M., On noise arising from the solar granulation. *Astrophys. J.* 1948, **107**, 1–5.
Singh, J., Hasan, S., Gupta, G., Nagaraju, K. and Banerjee, D., Spectroscopic observation of oscillations in the corona during the total solar eclipse of 22 July 2009. *Solar Phys.* 2011, **270**, 213–233.
Slater, L.J., *Confluent Hypergeometric Functions*, 1960 (Cambridge University Press: Cambridge). ISBN: 9781439834312.
Spruit, H.C., Motion of magnetic flux tubes in the solar convection zone and chromosphere. *Astron. Astrophys.* 1981, **98**, 155–160.
Spruit, H.C., Propagation speeds and acoustic damping of waves in magnetic flux tubes. *Solar Phys.* 1982, **75**, 3–17.
Srivastava, A.K., Zaqarashvili, T.V., Uddin, W., Dwivedi, B.N. and Kumar, P., Observation of multiple sausage oscillations in cool post-flare loop. *Mon. Not. Roy. Astron. Soc.* 2008, **388**, 1899–1903.
Stein, R.F. and Leibacher, J., Waves in the solar atmosphere. *Annu. Rev. Astron. Astr.* 1974, **12**, 407–435.
Stix, M., *The Sun. An Introduction*, 1989 (Springer Verlag: New York). ISBN:9780387500812.
Sturm, C., Mémoire sur les quations diffrentielles linaires du second ordre [Memory on linear differential equations of the second order]. *J. Math. Pures Appl.* 1836, **1**, 106–186.
Thomas, J.H., Magneto-atmospheric waves. *Annu. Rev. Fluid Mech.* 1983, **15**, 321–343.
Tian, H., McIntosh, S.W. and De Pontieu, B., The spectroscopic signature of quasi-periodic upflows in active region timeseries. *Astrophys. J.* 2011, **727**, L37–L43.
Tian, H., McIntosh, S.W., Habbal, S.R. and He, J., Observation of high-speed outflow on plume-like structures of the quiet sun and coronal holes with solar dynamics observatory/atmospheric imaging assembly. *Astrophys. J.* 2011, **736**, 130–140.
Tomczyk, S., McIntosh, S.W., Keil, S.L., Judge, P.G., Schad, T., Seeley, D.H. and Edmondson, J., Alfvén waves in the solar corona. *Science* 2007, **317**, 1192–1196.
Van Doorsselaere, T., Brady, C.S., Verwichte, E. and Nakariakov, V.M., Seismological demonstration of perpendicular density structuring in the solar corona. *Astron. Astrophys.* 2008, **491**, L9–L12.

Van Doorsselaere, T., Nakariakov, V.M. and Verwichte, E., Coronal loop seismology using multiple transverse loop oscillation harmonics. *Astron. Astrophys.* 2007, **473**, 959–966.
Van Doorsselaere, T., Nakariakov, V.M. and Verwichte, E., Detection of waves in the solar corona: Kink or Alfvén? *Astrophys. J.* 2008, **676**, L73–L75.
Verwichte, E., Marsh, M., Foullon, C., Van Doorsselaere, T., Moortel, I.D., Hood, A.W. and Nakariakov, V.M., Periodic spectral line asymmetries in solar coronal structures from slow magnetoacoustic waves. *Astrophys. J.* 2010, **724**, L194–L198.
Whittaker, E.T. and Watson, G.N., *A Course of Modern Analysis*, 1927 (Cambridge University Press: Cambridge). ISBN:9781603864541.
Yanowitch, M., Effect of viscosity on gravity waves and the upper boundary condition. *J. Fluid Mech.* 1977, **29**, 209–231.
Yuan, D. and Nakariakov, V.M., Measuring the apparent phase speed of propagating EUV disturbances. *Astron. Astrophys.* 2012, **543**, A9. ISSN: 0004-6361.
Yuan, D., Nakariakov, V.M., Chorley, N. and Foullon, C., Leakage of long-period oscillations from the chromosphere to the corona. *Astron. Astrophys.* 2011, **533**, A116. ISSN: 0004-6361.
Zhugzhda, Y.D. and Dzhalilov, N.S., Magneto-acoustic-gravity waves on the sun. I – exact solution for an oblique magnetic field. *Astron. Astrophys.* 1984, **132**, 45–51.

Appendix A. Solutions involving the confluent hypergeometric function of the second kind

The text has discussed the magnetosonic-gravity waves as a linear superposition (64) of two linearly independent solutions (63) expressible in terms of confluent hypergeometric functions of the first kind. Thus there was no need to consider the confluent hypergeometric of the second kind, that are also solutions of (60). For the sake of completeness, the solutions of (60) in terms of confluent hypergeometric functions of the second kind are considered in this appendix, and compared with the functions of the first kind. The confluent hypergeometric equation (49) with parameters $(1, b)$ has confluent hypergeometric function of the first kind (62) as one solution. Another linearly independent solution is (Carathéodory 1950, Lighthill 1977) the confluent hypergeometric function of the second kind:

$$\Gamma(b)G(b;1;\eta) = \mathrm{F}(b;1;\eta)\log\eta + \frac{\Gamma(b)}{\eta} + \mathrm{H}(b;1;\eta), \tag{A.1}$$

that consists of the sum of: (i) the function of the first kind (62) multiplied by a logarithmic singularity; (ii) another singular term corresponding to a pole with residue $\Gamma(b)$ where $\Gamma(...)$ is a Gamma function (Whittaker and Watson 1927, Campos 2014); (iii) a complementary function

$$\mathrm{H}(b;1;\eta) = \sum_{n=0}^{\infty} \frac{\eta^n}{n!} \frac{b(b+1)...(b+n-1)}{n!} [\psi(b+n) - 2\psi(1+n)], \tag{A.2}$$

where $\psi(...)$ is the digamma function (Copson 1935, Campos 2011a). Using (59a,b), (53a), (56), (50a,b) and (47a,c) leads to the vertical velocity perturbation spectrum of the magnetosonic-gravity waves

$$V^{\pm}(z;\omega) = \mathrm{e}^{z/2L} e^{\pm \mathrm{i}kz} \mathrm{G}\left(\frac{1}{2} \mp \frac{\mathrm{i}}{2\kappa} \pm \frac{\mathrm{i}}{2\kappa\gamma} \pm \frac{\mathrm{i}\kappa}{2\gamma}; 1; \mp \mathrm{i}\kappa\left(\beta + \frac{2}{\gamma} + \frac{z}{L}\right)\right), \tag{A.3}$$

which is similar to (63) replacing the confluent hypergeometric of the first by the second kind. Thus four solutions of the magnetosonic-gravity wave equation (45a,b) have been obtained, namely two involving confluent hypergeometric functions of the first (63) and second (A.3) kinds. Any two of the four functions $V_{\pm}$ in (63) and $V^{\pm}$ in (A.3) are linearly independent, and the general integral is a linear combination, justifying (64) as a legitimate choice involving only confluent hypergeometric functions of the first kind. Since these solutions are expansions

around the only singular point (52a,b), they have infinite radius of convergence and cover the whole altitude range, including the critical layer and the asymptotic limits at low and high altitude. In (63) and (A.3) were omitted some constant factors independent of z that can be absorbed in the constants of integration $A_\pm$ in (64). The critical layer corresponds, via (52a,b) and (59a), to the origin of the η-plane, where the confluent hypergeometric function of the first kind is unity (A.4a) and that of the second kind has a logarithmic singularity:

$$\mathrm{F}(b;1;\eta) = 1 + \mathrm{O}(\eta), \qquad \mathrm{G}(b;1;\eta) = \frac{\Gamma(b)}{\eta} + \log\eta[1+\mathrm{O}(\eta)] + \mathrm{O}(\eta). \tag{A.4a,b}$$

Thus a general solution finite at the critical layer is given by a linear combination (64) of confluent hypergeometric functions of the first kind. The asymptotic scaling at high $z \to +\infty$ and low $z \to -\infty$ altitude is considered next (appendix B) for both cases of solutions in terms of confluent hypergeometric functions of the first and second kinds.

Appendix B. Asymptotic wave fields at low and high altitude

The asymptotic form of the confluent hypergeometric function of the second kind is Abramowitz and Stegun (1964)

$$\mathrm{G}(b;1;\eta) = \eta^{-b}\sum_{n=0}^{N-1} b(b+1)...(b+n-1)(-\eta)^{-n} + \mathrm{O}(|\eta|^{-N}) \equiv J_1(b;1;\eta), \tag{B.1}$$

that may be designated first asymptotic function. The scaling at high $z \to +\infty$ or low $z \to -\infty$ altitude is given by

$$\eta^{-b} = (\pm \mathrm{i}q)^{-1/2\mp \mathrm{i}h}, \qquad q \equiv \beta + \frac{2}{\gamma} + \frac{z}{L}, \qquad h = \frac{1}{2\kappa} - \frac{1}{2\kappa\gamma} - \frac{\kappa}{2\gamma}. \tag{B.2a–c}$$

The complex expression (B.2a) (equivalent to (B.3)), namely

$$\begin{aligned}\eta^{-b} \equiv \exp\left[\log(\eta^{-b})\right] &= \exp(-b\log\eta) = \exp\left[\left(-\frac{1}{2} \mp \mathrm{i}h\right)\log(\pm \mathrm{i}q)\right] \\ &= \exp\left[\left(-\frac{1}{2} \mp \mathrm{i}h\right)\log\left(|q| \pm \mathrm{i}\frac{\pi}{2}\right)\right] \\ &= \exp\left[-\frac{1}{2}\log|q| + \frac{h\pi}{2} \mp \mathrm{i}\left(\frac{\pi}{4} + h\log|q|\right)\right],\end{aligned} \tag{B.3}$$

has modulus

$$|\eta^{-b}| = |q|^{-1/2}\exp\left(\frac{h\pi}{2}\right) \sim \left|\frac{L}{z}\right|^{1/2}, \tag{B.4}$$

showing that the waves are evanescent both at low $z \to -\infty$ and high $z \to +\infty$ altitude. Thus the solutions in terms of confluent hypergeometric functions of the second kind correspond to magnetosonic-gravity waves singular at the critical layer and vanishing at high and low altitude. The presence of a critical layer implies (Ince 1956) that the Sturm (1836) theorem does not apply, and a complete set of orthogonal eigenfunctions may not exist over the whole altitude range $]-\infty, +\infty[$. The extension to Klein and Körper (1881) theorem shows that two complete sets of orthogonal eigenfunctions exist in $]-\infty, 0[$ below and $]0, +\infty[$ above the critical layer, but they may not match across the critical layer.

The confluent hypergeometric function of the first kind has Slater (1960) the asymptotic expansion

$$\mathrm{F}(b;1;\eta)\sim\frac{\exp(\pm\mathrm{i}\pi b)}{\Gamma(1-b)}J_1(b;1;\eta)+J_2(b;1;\eta),\tag{B.5}$$

involving the first asymptotic function (B.1) and also the second asymptotic function,

$$J_2(b;1;\eta)=\frac{\mathrm{e}^\eta\eta^{b-1}}{\Gamma(b)}\sum_{n=0}^{N-1}(1-b)(2-b)...(n+1-b)\eta^{-n}.\tag{B.6}$$

The exponential term in the second asymptotic function (B.6) corresponds to upward and downward propagation:

$$\mathrm{e}^\eta=e^{\pm\mathrm{i}q}=\exp\left[\pm\mathrm{i}\left(\beta+\frac{2}{\gamma}+\frac{z}{L}\right)\right],\tag{B.7}$$

and does not affect the amplitude that is determined asymptotically by

$$\begin{aligned}\eta^{b-1}&\equiv\exp\left[(b-1)\log\eta\right]=\exp\left[\left(-\frac{1}{2}\pm\mathrm{i}h\right)\log(\pm\mathrm{i}q)\right]\\&=\exp\left[-\frac{1}{2}\log|q|-\frac{h\pi}{2}\mp\mathrm{i}\left(\frac{\pi}{4}-h\log|q|\right)\right],\end{aligned}\tag{B.8}$$

whose modulus scales:

$$|\eta^{b-1}|=|q|^{-1/2}\exp\left(-\frac{h\pi}{2}\right)\sim\left|\frac{L}{z}\right|^{1/2},\tag{B.9}$$

as (B.4) to within a constant factor. In conclusion: (i) the exponential amplitude growth and upward and downward propagation (56) apply to the vertical velocity perturbation of magnetosonic-gravity waves for all four solutions, namely the pairs (63) and (A.3) involving respectively confluent hypergeometric functions of the first (62) and second (A.2) kinds; (ii) any pair of the four solutions ($V_\pm$, $V^\pm$) is linearly independent, and the choice $V_\pm$ was made in the general integral (64); (iii) the choice of confluent hypergeometric functions of the first kind leads to finite wave fields at all altitudes whereas the second kind is singular at the critical layer; (iv) asymptotically at high $z\to+\infty$ and low $z\to-\infty$ altitude both confluent hypergeometric functions decay as $|z|^{-1/2}$ that is dominated by the $\exp(z/2L)$ factor in (63).